AN ABSTRACT OF THE THESIS OF

Donald J. Piepgras for the degree of Master of Science

in Geology presented on May 7, 1979

Title: THE ISOTOPIC COMPOSITION OF NEODYMIUM IN DIFFERENT OCEAN MASSES

Redacted for Privacy

Abstract approved _____

E. J. Dasch

Samarium-neodymium data for authigenic ferromanganese sediments from the oceans indicate that the Atlantic, Pacific, and Indian Oceans each have a distinct range in Nd isotopic composition, all of which are far less than $^{143}Nd/^{144}Nd$ ratios of source rocks with oceanic affinities. Direct measurements of the Nd isotopic composition of seawater presented here support the view that REE in ferromanganese sediments are derived by the direct precipitation of these elements out of seawater. Nd isotopic variations in ferromanganese sediments cannot be explained by contributions from continental detritus. It is therefore believed that the Nd isotopic variations found for ferromanganese sediments represent true variations in the isotopic composition of Nd dissolved in seawater in various ocean masses. These variations reflect primarily the age and $^{147}Sm/^{144}Nd$ of the continental masses being sampled, which is believed to be the major source of REE in seawater. These variations indicate that the residence time of Nd in seawater must be very short relative to the mixing rates between ocean masses. Nd isotopic studies, both in seawater and sediments should, therefore, be useful as a monitor of ocean currents and interocean mixing over the past several million years.

THE ISOTOPIC COMPOSITION OF NEODYMIUM IN DIFFERENT OCEAN MASSES

by

Donald J. Piepgras

A THESIS

Submitted to

Oregon State University

in partial fulfillment of
the requirements for the
degree of

Master of Science

June 1980

APPROVED:

Redacted for Privacy

Associate Professor of Geology in charge of major

Redacted for Privacy

Chairman, Department of Geology

Redacted for Privacy

Dean of Graduate School

Date thesis is presented on May 7, 1979

ACKNOWLEDGMENTS

I would like to thank Julius Dasch, my advisor, for getting me started in this project and providing me with financial support. The work has benefitted from discussions with Jack Dymond as well.

Special thanks are due to Dr. Jerry Wasserburg and other members of the Lunatic Asylum at Caltech for their support and technical expertise. Dr. Wasserburg has spent many long discussions with me, teaching me how to write a quality scientific paper, not to mention writing good English. Dimitri Papanastassiou spent a lot of time helping me to refine my mass spectrometer operational techniques as well as putting up with many of my silly questions. And most important, thanks go to Malcolm McCulloch, who sacrificed a great amount of his own time to teach me the ways of a "Lunatic," from being "clean" to instruction on chemical and mass spectrometric techniques. I have also benefitted from numerous discussions with Ted Wen, Stein Jacobsen, and Felix Oberli.

Don DePaolo allowed me to reproduce figures used in the appendices of this thesis from his Ph.D. thesis at Caltech. Portions of his thesis have been duplicated here for the benefit of the OSU mass spectrometry laboratory. These sections are on the chemistry and mass spectrometry techniques used at Caltech for Nd isotopic studies.

I am very grateful to Jack Corliss and Bobbi Conard for their contributions to my successful seawater experiments. Without their help, the work would never have been possible.

Samples used in this study were supplied by T. Walsh, J. Honnorez, J. Dymond, E. J. Dasch, F. Manheim, and K. Bruland.

Finally, I would like to thank Joanne Clark for typing this thesis, and the secretarial staff in the Lunatic Asylum for their valuable help in getting me through the "red tape" at Caltech.

This research has been supported by NSF grants from G. J. Wasserburg (Caltech), E. J. Dasch (OSU) and by a Geological Society of America Penrose Grant.

A portion of this thesis has been submitted for publication to Earth and Planetary Science Letters under the same title. This paper was co-authored by G. J. Wasserburg and E. J. Dasch. The inter-ocean mixing equations presented in this thesis were derived by G. J. Wasserburg for the paper submitted for publication.

TABLE OF CONTENTS

LIST OF FIGURES

LIST OF TABLES

THE ISOTOPIC COMPOSITION OF NEODYMIUM IN DIFFERENT OCEAN MASSES

INTRODUCTION

The purpose of this study was to determine the isotopic composition of Nd in the marine environment, and from the isotopic composition, to identify the sources of Nd in the different oceans. The Nd isotopic composition may have the possibility of serving as a natural tracer of ocean currents for short time scales and as a monitor of mixing in and between the oceans. The isotopic abundance of ^{143}Nd changes through geologic time due to the decay of ^{147}Sm ($\tau_{1/2} = 1.06 \times 10^{11}$ yrs). Observed $^{143}Nd/^{144}Nd$ ratios, therefore, reflect the age and $^{147}Sm/^{144}Nd$ ratio of the materials which are sampled. The average evolution of $^{143}Nd/^{144}Nd$ for the earth has been found to follow a simple growth curve which corresponds to the $^{147}Sm/^{144}Nd$ ratio of chondritic meteorites (1). However, terrestrial differentiation processes have segregated material into continental and oceanic crustal rocks with distinctive ages and Sm/Nd ratios. As a result, there is a clear difference in the $^{143}Nd/^{144}Nd$ ratios in the samples of different types of crustal rocks. Transport of the rare earth elements into the oceans will thus produce isotopic compositions of Nd which directly reflect the type of materials from which they were derived. The isotopic composition of Nd in the marine environment should therefore prove to be of interest in understanding the sources, transport, and deposition of REE in the oceans.

The residence time of Nd in seawater is believed to be short, less than 300 years (2), relative to the turnover rate for the oceans which is approximately 1000 years. Evidence for a short residence time can be demonstrated by comparing Na/Nd ratios for crustal rocks with that of seawater. Average crustal rocks have Na/Nd $\cong 10^3$ (Na $\cong$ 2.4%, Nd $\cong$ 28 ppm

[3]), while seawater has Na/Nd $\cong 3.5 \times 10^9$, six orders of magnitude higher than crustal rocks. The concentration of Nd in seawater is only 3×10^{-6} ppm (2,4 this study) compared with a Na concentration of 1.1% (5). This difference between seawater and crustal Na/Nd is clear evidence for a short residence time for Nd in seawater.

In this study, $^{143}Nd/^{144}Nd$ and $^{147}Sm/^{144}Nd$ were measured in metal rich authigenic sediments from the major oceans. Samples include manganese nodules, hydrothermal crusts, and metalliferous sediments. It is generally believed that the metals and REE in these sediments precipitate directly out of seawater (2, 6-11), although some nodules exhibit REE patterns that are quite fractionated relative to the observed average REE pattern in seawater (8, 12, 13). This observation has been used as evidence against direct precipitation from seawater. However, variations of REE patterns may result entirely from fractionation during precipitation and not directly reflect the patterns of the source. In either case, the isotopic abundance of Nd would be unaffected by the precipitation process and, therefore, variations in the $^{143}Nd/^{144}Nd$ ratio will be a direct result of the isotopic abundance of Nd dissolved in seawater with possible contributions from marine rocks, sediments, and detrital materials. As the isotopic composition of Sr is rather uniform in seawater, we have tested for detrital contributions by measuring $^{87}Sr/^{86}Sr$ ratios in some of the same samples analyzed for Nd.

In addition to measurements on authigenic sediments, we also present direct measurement of the Nd isotopic composition for three seawater samples from the Pacific Ocean. These measurements give the present day $^{143}Nd/^{144}Nd$ values in a given water mass, whereas data

on deep ocean manganese nodules give values which can represent an average over several millions of years. The direct Nd isotopic measurements on seawater also afford greater confidence in interpretation of the sediment data and aids in answering questions regarding the derivation of REE in ferromanganese sediments.

Previous studies have shown that the isotopic composition of Nd in oceanic basalts is distinctly different from that in average continental rocks (1, 14, 15, 16). The Nd isotopic composition of seawater must be a result of mixing of Nd from these two sources. A preliminary attempt to estimate the isotopic composition of Nd in seawater was made by DePaolo and Wasserburg (17) using fish debris. A more extensive study was presented by O'Nions *et al.* (18) who measured Nd in manganese nodules and metalliferous sediments. While substantial variations were found, O'Nions *et al.* inferred that seawater had a uniform $^{143}Nd/^{144}Nd$ ratio and that variations were dominately due to inclusion of detrital components. The present study will show that there is a wide spread in $^{143}Nd/^{144}Nd$ in authigenic sediments in support of previous observations but will attempt to show that this variation is due to isotopic differences in Nd dissolved in seawater as a result of the ages and $^{147}Sm/^{144}Nd$ ratios of the continental mass supplying Nd to a given seawater mass.

SAMPLES

Marine ferromanganese sediments were used in this study because they (1) occur in relative abundance over a wide geographic range, (2) form in a variety of depositional environments, (3) apparently form primarily by authigenesis, commonly with minimal amount of included detritus, and (4) have high rare earth element concentrations. There are several types of

ferromanganese sediments which are classified according to their depositional environment as summarized by Bonatti et al. (7). We have sampled two types of ferromanganese deposits, classified as hydrogenous and hydrothermal. Samples were selected from major ocean basins and mid-ocean ridge spreading centers. Locations are given in Table 1 and Figure 1.

Manganese nodules comprise the bulk of hydrogenous ferromanganese sediments. The assumption leading to the selection of manganese nodules was that their REE precipitate directly out of seawater, and therefore their Nd isotopic composition would represent that of the seawater from which they were derived. Support for the hypothesis of seawater derivation for REE in manganese nodules comes from many authors (2, 7, 8, 19, 20). Erlich (12) and Bender (13) prefer a mechanism of diagenetic remobilization of REE from underlying sediments as a source for these elements. This has been argued for other elements as well (7, 21, 22, 23, and others). Many nodules are also characterized by the presence of clay and other particles dispersed throughout their structures (24). These latter features, if detrital, could have a significant effect on elemental composition, possibly including Nd. In addition to Nd dissolved in seawater, other possible sources which could affect the Nd isotopic composition in the samples include continental detritus, oceanic basalts and sediments, and juvenile material.

Samples were chosen to achieve two main objectives: 1) to establish differences or similarities in Nd isotopic composition between various water bodies, and 2) to determine if variations exist within a body of water, which may be related to differences in provenance. To meet these objectives, broad geographic sampling of nodules within the

Table 1. Sample locations and Sm and Nd results.

Sample #	Lab.#[a]	Sample Location	Nd ppm	Sm ppm	$\frac{^{147}Sm}{^{144}Nd}$	$\frac{^{143}Nd}{^{144}Nd}$[b]
I. Pacific Ocean						
OC73-3-12P	MS-1	20°22'12"S, 112°19'12"W	20.7	5.01	0.146	0.511780±20
OC73-3-12MG3	MS-2a	20"43'12"S, 112°27'00"W	15.7	3.60	0.137	0.511633±28
Duplicate	Ms-2b	" "	16.5			0.511659±25[c]
52DR5	HC-1	00°36'N, 86°06'W	2.05	0.39	0.115	0.511769±26
MD1-1-1Top	MN-1	31°N, 155°W	196	50.0	0.153	0.511618±15
MD1-1-1Bottom	MN-2	31°N, 155°W	129	33.1	0.155	0.511620±28
DWHD-47	MN-3	41°59'S, 102°01'W	175	42.5	0.146	0.511611±22
Antp 58D	MN-4	18°57'N, 135°48'E	225	51.4	0.138	0.511565±37
SCAN 35D	MN-5	20°55'N, 142°22'E	143	32.7	0.138	0.511656±25
CEROP II 1000m DISS	SW-1	36°47'N, 122°48'W	3.2×10^{-6}	0.63×10^{-6}	0.118	0.511641±36[c]
CEROP II 2400m DISS	SW-2	36°50'N, 122°50'W	-	-	-	0.511712±25
CEROP II 1000m DISS	SW-3	36°47'N, 122°48'W	-	-	-	0.511718±25
II. Atlantic Ocean						
CYP74-12	HC-2	36°56'N, 33°04'W	4.45	1.01	0.136	0.511245±32
S-M	MN-6	33°57'N, 65°47'W	179	45.1	0.152	0.511223±21

Table 1. (continued)

Sample #	Lab.#[a]	Sample Location	Nd ppm	Sm ppm	$\frac{147_{Sm}}{144_{Nd}}$	$\frac{143_{Nd}}{144_{Nd}}$[b]
II. Atlantic Ocean (continued)						
BP-2381	MN-7	31°04'12"N, 78°08'30"W	107	23.1	0.129	0.511273±22
BP-2382	MN-8	31°01'36"N, 78°18'48"W	59.4	14.2	0.145	0.511312±42
VEMA FRACTURE ZONE	MN-9	10°53'42"N, 45°17'48"W	155	38.5	0.149	0.511293±18
CIRCE 244D	MN-10	08°22'S, 13°13'W	233	59.6	0.154	0.511216±18
CHN115 Sta 146	MN-11a	30°12'48"S, 39°21'30"W	250	56.2	0.135	0.511118±38
" "	MN-11b	" "	"	"	"	0.511117±22
III. Indian Ocean						
DODO 127D	MN-12	06°40'01"S, 51°54'00"E	199	44.0	0.133	0.511432±26
Antp 109D	MN-13	29°58'23"S, 60°47'49"E	169	38.7	0.138	0.511404±31
DODO 232D	MN-14	05°22'59"S, 97°28'59"E	262	68.6	0.158	0.511465±29
DODO 62D	MN-15	16°18'00"S, 104°16'01"E	90.3	22.5	0.150	0.511461±24
PCE 55-31	MN-16	36°27'07"S, 110°02'24"E	134	30.3	0.136	0.511281±46
DODO 62D Sed	RC-1	16°18'00"S, 104°16'01"E	33.0	8.31	0.152	0.511350±25
IV. Antarctic Ocean						
BT-14-3	MN-17	56°13'S, 164°20'W	67.2	17.4	0.156	0.511500±30

Table 1. (continued)

Sample #	Lab.#[a]	Sample Location	Nd ppm	Sm ppm	$\frac{^{147}Sm}{^{144}Nd}$	$\frac{^{143}Nd}{^{144}Nd}$[b]
V. Scotia Sea						
E28-5	MN-18	57°54'S, 57°00'W	63.0	14.2	0.136	0.511567±28
VI. Lake Oneida, NY - Lacustrine						
Lake Oneida, NY	MN-19	43°10'N, 75°45'W	34.0	9.19	0.163	0.511281±29

[a] MN = manganese nodule MS = metalliferous sediment HC = hydrothermal crust RC = Red clay SW = seawater

[b] Data normalized to $^{150}Nd/^{142}Nd = 0.2096$.

[c] Spiked with ^{150}Nd and normalized to $^{146}Nd/^{142}Nd = 0.636155$.

FIGURE 1

Locations of samples analyzed in this study. Also included are manganese nodule and metalliferous sediment sites from O'Nions et al. (18) (A-50D, D-3D, B-15P, V-19-53, F-55-16-1) and a red clay (DSDP37-3-2) from McCulloch and Wasserburg (36).

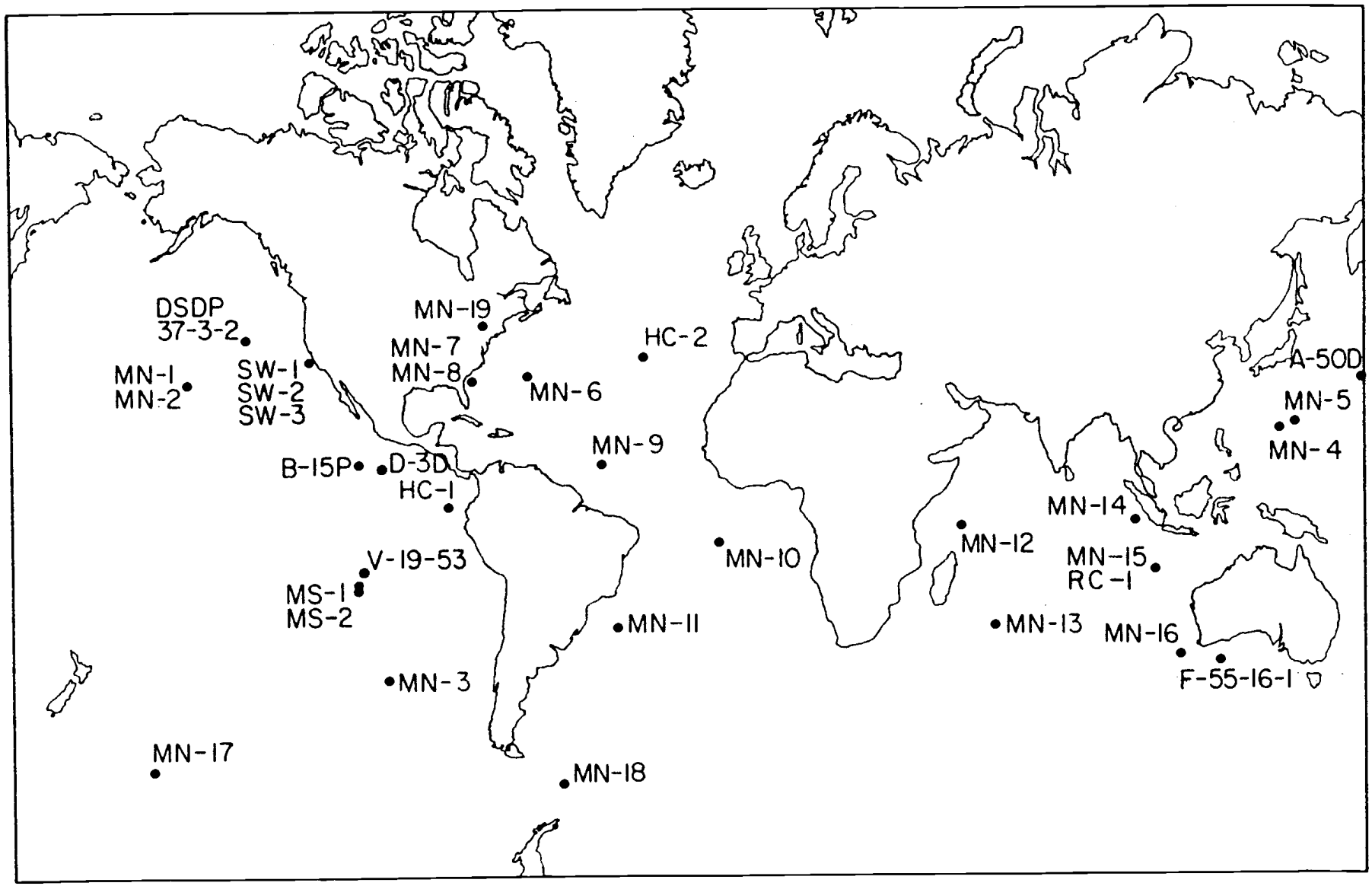
DSDP
37-3-2
MN-1
MN-2
SW-1
SW-2
SW-3
MN-19
MN-7
MN-8
MN-6
HC-2
A-50D
MN-5
MN-4
MN-9
B-15P
D-3D
HC-1
MN-14
MN-12
MN-10
MN-15
RC-1
V-19-53
MS-1
MS-2
MN-11
MN-13
MN-16
F-55-16-1
MN-3
MN-17
MN-18

FIGURE 1

Atlantic, Pacific, and Indian Oceans were made (Figure 1). Samples from the Scotia Sea and Antarctic Ocean were chosen as representing locations where mixing between two different water masses may be taking place. A manganese nodule and an associated red clay from the Indian Ocean (RC-1 and MN-15) were analyzed to compare the Nd isotopic composition between manganese nodules and the underlying sediment substrate in the same area. In addition, one lacustrine nodule from Lake Oneida, New York, was analyzed. This latter sample was chosen on the assumption that all of its REE were continentally derived.

Two types of hydrothermal samples have also been sampled. These are hydrothermal crusts and metalliferous sediments. Samples were chosen to determine if there were effects due to hydrothermal activity on the Nd isotopic composition. The direct association of these deposits with hydrothermal activity and their rapid rate of deposition (25, 26, 27) make them genetically distinct from manganese nodules. These deposits are believed to form by direct precipitation out of seawater (6, 7, 10, 11, 25, 28, and others). While iron and manganese have been shown by these authors to have a source related to hydrothermal alteration of basalts, this has not been clearly established for the rare earth elements. Corliss (11) studied altered oceanic basalts and concluded that REE in marine sediments could be accounted for by derivation from the basalts. However, REE patterns for hydrothermal deposits are similar to seawater REE patterns and not basalt, leading many authors to conclude their REE were derived from seawater (25, 29, 30). Nd isotopic analyses were made on metalliferous sediments from the East Pacific Rise, and on hydrothermal crusts from the Galapagos hydrothermal mounds and the FAMOUS site on the mid-Atlantic Ridge in an attempt to clarify their origin.

Finally, we have attempted to make a direct determination of the Nd isotopic composition of seawater. Three seawater samples were obtained which were collected from the Pacific Ocean by K. Bruland during the CEROP II expedition of the Oregon State University's RV Wecoma. Samples were collected at approximately 1000 m (SW-1, SW-3) and 2400 m (SW-2) depths from a location offshore from Monterey, California (Figure 1, Table 1). SW-1 and SW-3 are separate aliquots of the same water sample.

ANALYTICAL PROCEDURES AND DATA REPRESENTATION

Ferromanganese sediment samples were treated with 4.0 N HCl for the dissolution of the authigenic materials. A few samples were also treated with 1 ml 1:1 HF and $HClO_3$. The estimated mass of residue remaining after dissolution by these two methods were the same. Typical sample sizes were about 15 mg to 20 mg. Samples were either aliquots of a powdered sample or, where available, intact nodules. Surfaces of intact nodules were first stripped of surface layers, about 1-2 mm, and the sample then was scraped from the clean surface below. Chemical separation and mass spectrometry of Sm and Nd have been described elsewhere (1, 31). Sm and Nd concentrations were determined by isotope dilution on sample aliquots. Strontium and neodymium were separated by our standard ion exchange techniques (32) with typical blank levels of 100×10^{-12} gm and 60×10^{-12} gm respectively.

Seawater analyses were carried out on the REE fraction separated from $1.0\text{-}2.0 \times 10^{4}$ gm of seawater which was filtered on board the RV Wecoma through acid cleaned, 142 mm diameter nucleopore filters with a pore size of 0.4 μm. Our Sm-Nd separations and analyses were done on REE

fractions prepared by Roberta Conard at Oregon State University following the procedure summarized below. Samples were acidified in the laboratory to pH $\cong$ 1.5 and set aside for one week. The REE were precipitated from the seawater using the method described by Goldberg et al. (2). High purity Fe_2O_3 powder dissolved in 6.0 N HCl is added to the water samples. The iron was precipitated as $Fe(OH)_3$ by bybbling NH_3 gas through the water until a pH of 9.0 was attained; the REE were adsorbed onto these reactive surfaces. This procedure has typical REE yields of about 90% as determined from the activity of ^{170}Tm added to the samples prior to precipitation. Precipitates were then transferred to Caltech to separate Sm and Nd. The total chemistry blank for this separation of Nd was determined on a sample of reagents prepared in the same proportions as were used for the separation of REE from the seawater samples. The contribution from these reagents was found to be about 0.3×10^{-9} gm of Nd, which comprises less than 1% of the total Nd yield.

The isotopic abundance of all the Nd isotopes were measured in every experiment and, with the exception of the three seawater samples were found to be in excellent agreement with values measured by DePaolo and Wasserburg (1). An excess of ^{148}Nd, measured as $^{148}Nd/^{144}Nd$, was found in each of the seawater samples ranging from approximately 15 to 27 ε units (Table 2) relative to the normal abundance of this isotope as has been measured in the ferromanganese sediments. This excess of the $^{148}Nd/^{144}Nd$ occurs with or without the use of ^{170}Tm tracer (samples SW-1, SW-2) which was added to determine REE precipitation yields and ^{147}Sm and ^{150}Nd tracers added to determine Sm and Nd concentrations (SW-1 only). All other isotopes of Nd have normal abundances. A REE carrier solution is used routinely in the laboratory where

Table 2. $\varepsilon_{Nd}(0)$ values for stable Nd isotopes in seawater samples

Lab. #	$\varepsilon_{^{142}Nd}(0)^c$	$\varepsilon_{^{145}Nd}(0)^c$	$\varepsilon_{^{146}Nd}(0)^c$	$\varepsilon_{^{148}Nd}(0)^c$
SW-1[a]	-0.7 ±0.5	-2.2 ±1.4	-	+26.6 ± 1.4
SW-2[b]	+0.7 ±0.5	-0.5 ±0.5	-0.6 ±0.5	+18.9 ±0.8
SW-3[b]	+1.0 ±0.5	-0.9 ±1.0	-0.8 ±0.8	+14.7 ±1.7

[a] Spiked with ^{150}Nd and normalized to $^{146}Nd/^{142}Nd = 0.636155$.

[b] Normalized to $^{150}Nd/^{142}Nd = 0.2096$.

[c] Normal isotopic abundances have $\varepsilon_{Nd}(0) = 0$.

the REE were precipitated from the seawater samples, for the purpose of determining chemistry yields on seawater REE samples measured by neutron activation analysis (see Goldberg et al. [2]). This REE carrier solution contains enriched ^{148}Nd as well as other REE, and it therefore seems plausible that the $^{148}Nd/^{144}Nd$ excess we observe may be due to cross contamination inadvertently introduced to our samples from this carrier. ^{148}Nd is not used for fractionation corrections, so we are confident that all the other Nd isotope ratios measured in the seawater samples are unaffected by contamination.

Samples of Nd were analyzed on the Lunatic I mass spectrometer (33) as NdO^+. Sample sizes for ferromanganese sediments were 200-300 x 10^{-9} gm Nd. Typical ion beam intensities at mass 160($^{144}Nd^{16}O$) were 8.0 x 10^{-12} A. This beam intensity was maintained for 6-8 hours while approximately 200 ratios were measured for each sample. Seawater samples sizes were less than 50 x 10^{-9} gm Nd. With the exception of SW-1, ion beam intensities were the same as those for ferromanganese samples just mentioned. SW-1 was analyzed at an ion beam intensity of 4.0 x 10^{-12} A. About 200 ratios were measured for each water sample.

Representation of Sm, Nd and Sr data follows that given by DePaolo and Wasserburg (1, 17). Measured $^{143}Nd/^{144}Nd$ ratios are presented as fractional deviations in parts in 10^4 (ε units) from $^{143}Nd/^{144}Nd$ in a chondritic uniform reservoir (CHUR) as measured today

$$\varepsilon_{Nd}(0) = \left[\frac{(^{143}Nd/^{144}Nd)_M}{I_{CHUR}(0)} - 1 \right] \times 10^4$$

where M is the ratio measured in the sample today, and $I_{CHUR}(0) = 0.511836$ is the $^{143}Nd/^{144}Nd$ in the CHUR reference reservoir today. Similarly,

an enrichment factor for $^{147}Sm/^{144}Nd$ in a sample relative to CHUR is given by

$$f_{Sm/Nd} = \left[\frac{(^{147}Sm/^{144}Nd)_M}{(^{147}Sm/^{144}Nd)_{CHUR}} - 1 \right]$$

where $(^{147}Sm/^{144}Nd)_{CHUR} = 0.1936$. - Model ages, T^{Nd}_{CHUR}, are calculated for the samples as follows

$$T^{Nd}_{CHUR} = \frac{1}{\lambda} \ell n \left[1 + \frac{\varepsilon_{Nd}(0)\ I_{CHUR}(0) \times 10^{-4}}{f_{Sm/Nd}(^{147}Sm/^{144}Nd)_{CHUR}} \right]$$

The ^{147}Sm decay constant, $\lambda = 6.54 \times 10^{-12}\ yr^{-1}$. Errors reported for T^{Nd}_{CHUR} model ages are typically less than 10% and only include the errors in $\varepsilon_{Nd}(0)$. Sr isotopic data is presented in a manner analogous to that used for Sm-Nd data. Thus,

$$\varepsilon_{Sr}(0) = \left[\frac{(^{87}Sr/^{86}Sr)_M}{I_{UR}(0)} - 1 \right] \times 10^4$$

where $I_{UR}(0) = 0.7045$ is the estimated $^{87}Sr/^{86}Sr$ value for the bulk earth as determined by DePaolo and Wasserburg (14) and O'Nions et al. (15).

RESULTS

Results of Nd isotopic analyses are given in Tables 1 and 3 and Figure 2. All samples measured have $\varepsilon_{Nd}(0)$ less than -1 and range as low as -14. Figure 2 clearly shows that these samples lie well below typical values observed for oceanic igneous rocks such as mid-ocean ridge, oceanic island, and island arc basalts. We note, however, that our data lie between (and overlap to some extent) typical values for continental flood basalts and average crustal rocks. Clearly, these data show that the dominant contribution to the rare earth elements in these samples is from

the continents and not from rocks with oceanic crust or mantle affinities. Furthermore, we observe from Figure 2 a distinct clustering of isotopic data from the Pacific, Indian, and Atlantic Oceans. Samples associated with each water mass occupy an isotopically distinct range, with the Atlantic Ocean data as the most negative, the Pacific Ocean the least negative, and the Indian Ocean having intermediate values. Only one sample, MN-16 from the Indian Ocean, overlaps the range defined by samples from another ocean. This regular pattern is independent of the nature of the material analyzed.

Pacific Ocean: Samples analyzed from the Pacific Ocean occupy a narrow range of $\varepsilon_{Nd}(0)$ from -1.1 to -4.4. This is in excellent agreement with previous data from O'Nions et al. (18) for Pacific samples. Manganese nodules range from -2.6 to -4.4, including data from O'Nions et al. Top and bottom material from an apparently unturned manganese nodule (MN-1, MN-2) have identical Nd isotopic compositions, although the topmost sample has about a factor of 2 higher concentration of both Sm and Nd. We note that two metalliferous sediment samples from the East Pacific Rise (MS-1, this study, and V-19-53(40), O'Nions et al. [18] and the Galapagos hydrothermal crust (HC-1) exhibit the least negative values observed and are distinctly separated from the bulk of Pacific samples. We also note that the average $\varepsilon_{Nd}(0)$ value for three seawater samples is about -2.8 and lies in the range defined by the ferromanganese sediments.

Atlantic Ocean: $\varepsilon_{Nd}(0)$ values for Atlantic samples are distinctly different from Pacific samples. Values range from -10.2 to -14.0, with the bulk of the samples lying between -10.2 and -12.1. One sample (HC-2) is a manganese-rich crust from the project FAMOUS site in the North Atlantic. It has $\varepsilon_{Nd}(0) = -11.5$ and it is indistinguishable from most

Table 3. Nd evolutionary parameters.

	Lab.#	$\varepsilon_{Nd}(0)$	$f_{Sm/Nd}$	$T^{Nd}_{CHUR\ AE}$
I. Pacific Ocean				
	MS-1	-1.1±0.4	-0.246	0.18
	MS-2a	-4.0±0.6	-0.292	0.55
	MS-2b	-3.5±0.5		
	HC-1	-1.4±0.5	-0.408	0.14
	MN-1	-4.3±0.3	-0.208	0.83
	MN-2	-4.2±0.5	-0.199	0.85
	MN-3	-4.4±0.4	-0.245	0.72
	MN-4	-4.3±0.7	-0.289	0.60
	MN-5	-3.5±0.5	-0.290	0.49
	SW-1	-3.8±0.7	-0.393	0.39
	SW-2	-2.4±0.5	-	-
	SW-3	-2.3±0.5	-	-
II. Atlantic Ocean				
	HC-2	-11.5±0.6	-0.296	1.57
	MN-6	-12.0±0.4	-0.217	2.21
	MN-7	-11.0±0.4	-0.334	1.32
	MN-8	-10.2±0.8	-0.258	1.60
	MN-9	-10.6±0.4	-0.229	1.86
	MN-10	-12.1±0.4	-0.204	2.38
	MN-11a	-14.0±0.7	-0.301	1.87
	MN-11b	-14.0±0.4	-0.301	1.88
III. Indian Ocean				
	MN-12	-7.8±0.5	-0.313	1.01
	MN-13	-8.5±0.6	-0.287	1.19
	MN-14	-7.3±0.6	-0.184	1.58
	MN-15	-7.3±0.5	-0.224	1.32
	MN-16	-10.8±0.9	-0.297	1.47
	RC-1	-9.5±0.5	-0.215	1.77
IV. Antarctic Ocean				
	MN-17	-6.6±0.6	-0.197	1.34
V. Scotia Sea				
	MN-18	-5.3±0.5	-0.298	0.72
VI. Lake Oneida, NY				
	MN-19	-10.9±0.6	-0.159	2.73

FIGURE 2

Histogram of $\varepsilon_{Nd}(0)$ of marine ferromanganese sediments and seawater measured in this study. Data from O'Nions et al. (18), renormalized to $^{150}Nd/^{142}Nd = 0.2096$, has been included. Data on continental and oceanic rocks have been adapted from DePaolo and Wasserburg (17).

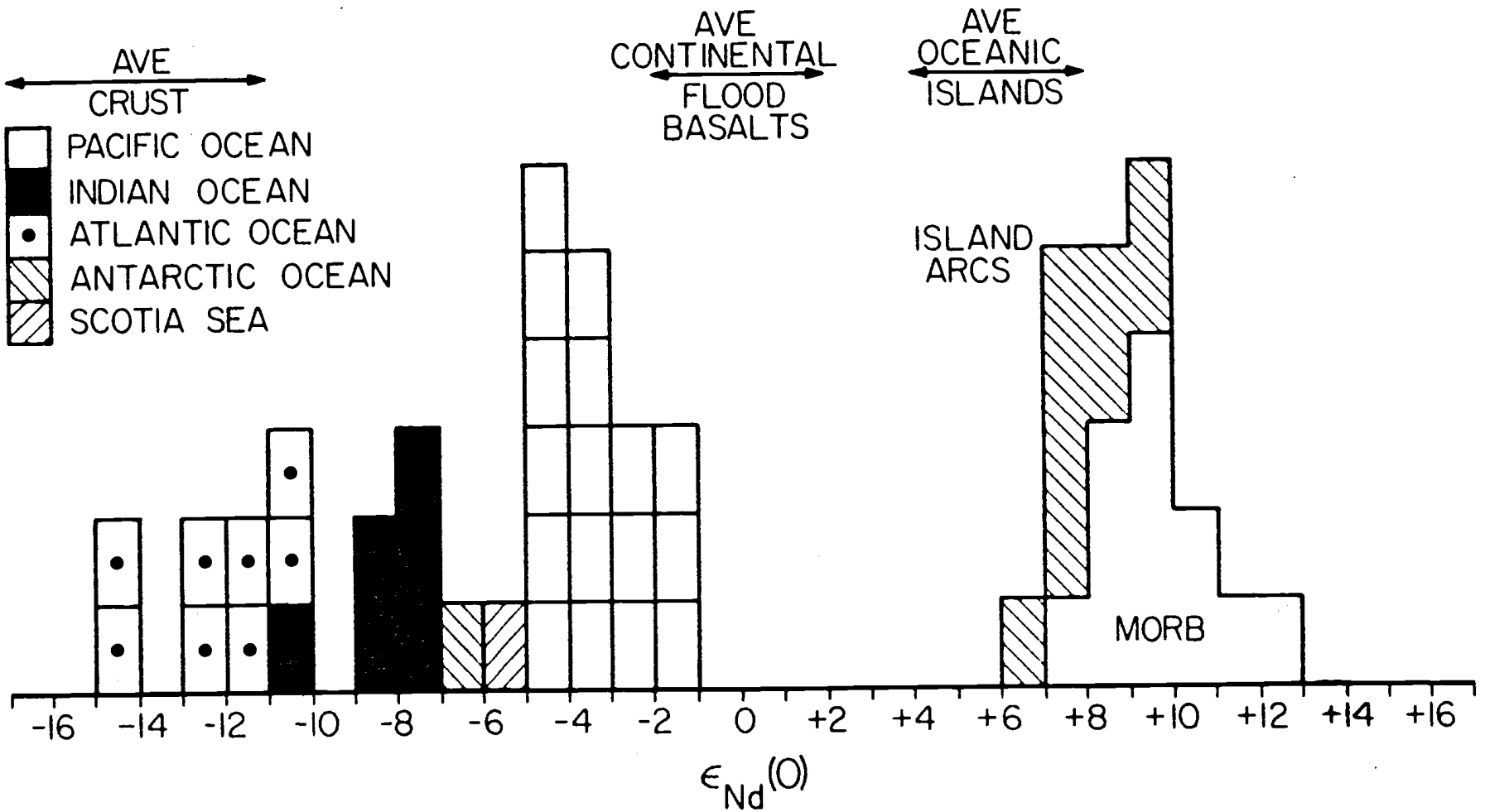
AVE
CRUST
PACIFIC OCEAN
INDIAN OCEAN
ATLANTIC OCEAN
ANTARCTIC OCEAN
SCOTIA SEA
AVE
CONTINENTAL
FLOOD
BASALTS
AVE
OCEANIC
ISLANDS
ISLAND
ARCS
MORB
-16 -14 -12 -10 -8 -6 -4 -2 0 +2 +4 +6 +8 +10 +12 +14 +16
$\epsilon_{Nd}(0)$

FIGURE 2

other Atlantic samples which consist of manganese nodules. Samples MN-11a and b are duplicate analyses of a nodule from the South Atlantic. Their $\varepsilon_{Nd}(0)$ values of -14.0 are the most negative reported.

Indian Ocean: Five manganese nodules have been analyzed. With the exception of MN-16, $\varepsilon_{Nd}(0)$ values lie between -7.3 and -8.5, approximately midway between Pacific and Atlantic sample values. Previous data from O'Nions et al. (18) for an Indian Ocean nodule also lies in this range. MN-16 has $\varepsilon_{Nd}(0) = -10.8$ which is more typical of Atlantic samples. A deep sea red clay (bulk sample, untreated) from the Indian Ocean (RC-1) is also more negative than the bulk of the reported data for this ocean ($\varepsilon_{Nd}(0) = -9.5$).

Other samples: Two nodules from southern oceans, the Scotia Sea and the Antarctic Ocean, have $\varepsilon_{Nd}(0)$ values which lie between those observed for the Pacific and Indian Oceans. MN-19 from Lake Oneida has $\varepsilon_{Nd}(0) = -10.9$ which is within the range of data for Atlantic samples.

Four manganese nodules and one metalliferous sediment were also analyzed for $^{87}Sr/^{86}Sr$. Results of these measurements are given in Table 4. All samples have $\varepsilon_{Sr}(0)$ indistinguishable from seawater ($\varepsilon_{Sr}(0) = +65.0$) in spite of a wide range in $\varepsilon_{Nd}(0)$ and geographic location.

DISCUSSION

Neodymium isotopic data for ferromanganese nodules, hydrothermal crusts, and metalliferous sediments exhibit distinctive and tightly clustered $\varepsilon_{Nd}(0)$ values within each of the major oceans analyzed. This is in sharp contrast with the $^{87}Sr/^{86}Sr$ isotopic composition of these sediments which is uniform in all samples studied and is identical to that of dissolved Sr in modern seawater. The Atlantic Ocean has the most negative

Table 4. Nd and Sr evolutionary parameters for selected samples

Lab.#	$^{143}Nd/^{144}Nd$	$^{87}Sr/^{86}Sr$[a]	$\varepsilon_{Nd}(0)$	$\varepsilon_{Sr}(0)$
MS-2	0.511633 ±28	0.709040 ±37	-4.0 ±0.6	+64.4 ±0.7
MN-7	0.511273 ±22	0.709030 ±40	-11.0 ±0.4	+64.3 ±0.8
MN-10	0.511216 ±18	0.709068 ±37	-12.1 ±0.4	+64.8 ±0.8
MN-15	0.511461 ±24	0.709090 ±60	-7.3 ±0.5	+65.2 ±1.2
MN-3	0.511611 ±22	0.709015 ±40	-4.4 ±0.4	+64.1 ±0.8
Seawater[b]		0.70909		+65.2

[a]Data normalized to $^{86}Sr/^{88}Sr = 0.1194$.

[b]Average of values measured on the Caltech Sr seawater standard (42).

values (average $\varepsilon_{Nd}(0) \cong -12$), the Indian Ocean has intermediate values (average $\varepsilon_{Nd}(0) \cong -8$), and the Pacific Ocean has the least negative values (average $\varepsilon_{Nd}(0) \cong -3$). Data for samples from each ocean show relatively small dispersion about the respective average $\varepsilon_{Nd}(0)$ values, with a maximum spread of only ±2 ε units in each ocean. The possible sources for REE which could contribute to these sediments include: dissolved REE from continental sources, dissolved REE from marine sources, detrital debris from continental materials and debris from oceanic igneous rocks and sediments. Some of the oceanic sources (e.g., marine hydrothermal solutions) could in principle cause major changes in the local contribution of REE. Some mixture of REE from these sources determines the Nd isotopic composition of ferromanganese sediments in each ocean, and some small variation in the proportions of these individual components must be responsible for the small variations with an ocean. The observed Nd uniformities in each ocean indicate that contributions to this element are relatively well mixed and distinctly different for each major water mass.

Nd isotopic uniformity for ferromanganese sediments from each of the oceans is maintained despite many factors and genetic variables. Concentration of Nd shows no correlation with isotopic composition. Nd concentrations vary by more than two orders of magnitude in nodules and metalliferous sediments from the Pacific Ocean, and somewhat less in the Atlantic. In spite of this variation, all samples maintain nearly the same Nd isotopic composition within the same ocean. Further, the highly variable accumulation rates of ferromanganese sediments do not appear to cause any effects on Nd isotopic composition, as manganese nodules have

extremely slow growth rates of a few millimeters per 10^6 years (34, 35), whereas hydrothermal crusts may grow as fast as 2 mm/1000 years (26, 27). Possible contributions to manganese nodules from diagenetically remobilized REE from underlying sediments also has no large local effects on $\varepsilon_{Nd}(0)$. If diagenetic remobilization is a significant source of REE in manganese nodules, then underlying deep sea sediments must also be characterized by Nd isotopic values which are close to that of the ocean basin. Deep sea red clays (RC-1, DSDP37-3-2 [36]) have $\varepsilon_{Nd}(0)$ values similar to ferromanganese sediments in the same ocean, but the data base is too limited to draw any conclusions regarding their sources.

Nd isotopic measurements of Pacific seawater samples show a strong similarity to Pacific ferromanganese sediments. Seawater, with $\varepsilon_{Nd}(0)$ values falling about midway in the spread exhibited by ferromanganese sediments, leads us to the conclusions that the source of Nd in Pacific ferromanganese sediments is from Nd dissolved in seawater, and that Pacific seawater is isotopically rather uniform with respect to Nd. These conclusions, coupled with the previous discussion on the isotopic uniformity of ferromanganese sediments in each ocean, lead us to infer that the Nd isotopic composition of seawater in the Atlantic, Indian, and Pacific Oceans are distinctly different from each other, but fairly uniform within each ocean. To test these conclusions directly, Nd isotopic measurements of a variety of seawater samples will have to be made.

In a previous study, O'Nions *et al.* (18) reported the Nd isotopic composition in ferromanganese nodules to be variable but concluded that the value of Nd in seawater was $\varepsilon_{Nd}(0) \cong -3$. These workers attributed the variability to detritus included in the nodules but considered their data on Pacific nodules to be more representative of seawater. This was a

reasonable conclusion, because $^{87}Sr/^{86}Sr$ measured in their Indian Ocean nodule was distinctly greater than the $^{87}Sr/^{86}Sr$ ratio for dissolved Sr in seawater. However, the Nd values reported by O'Nions et al. (18) for samples from each ocean lie well within the groupings reported here, yet our $^{87}Sr/^{86}Sr$ ratios are all identical to modern seawater $^{87}Sr/^{86}Sr$ ratios in spite of variable $\varepsilon_{Nd}(0)$ values. The conclusions by O'Nions et al. (18) reflects their more limited data base, the absence of a consideration of residence times for REE, as well as the magnitude of possible detrital contributions.

To assess the effects of detrital contributions, consider mixtures (m) of two components A and B. The Nd composition is given by

$$\varepsilon^{m}_{Nd}(0) = \frac{(X_A)(C^{A}_{Nd})(\varepsilon^{A}_{Nd}(0)) + (1-X_A)(C^{B}_{Nd})(\varepsilon^{B}_{Nd}(0))}{(X_A)(C^{A}_{Nd}) + (1-X_A)(C^{B}_{Nd})} \qquad (1)$$

where X_A is the weight fraction of component A and C^{A}_{Nd} and C^{B}_{Nd} are the concentrations of Nd (in ppm) in components A and B. If we take the shift between Atlantic and Pacific samples to represent a detrital component (B) added to a seawater component (A) with $\varepsilon^{A}_{Nd}(0) \cong -3$, we can calculate the value of $\varepsilon^{B}_{Nd}(0)$ in the detrital component. We use $(1-X_A) = 0.2$ as a reasonable limit on the weight fraction of detrital material in a manganese nodule (based on world averages for Al and Si abundances in nodules [37]) and a low value of $C^{A}_{Nd} = 100$ ppm Nd in the uncontaminated nodule. This yields

$$[\varepsilon^{B}_{Nd}(0) - \varepsilon^{m}_{Nd}(0)]\, C^{B}_{Nd} = \frac{X_A\, C^{A}_{Nd}}{(1-X_A)} [\varepsilon^{m}_{Nd}(0) - \varepsilon^{A}_{Nd}(0)]$$

$$\cong 3.6 \times 10^{3} \text{ (units of ppm)}$$

for the Atlantic Ocean where $\varepsilon^{m}_{Nd}(0) \cong -12$. For $C^{B}_{Nd} \cong 35$ ppm, a high

value for most crustal rocks, this yields $\varepsilon^{B}_{Nd}(0) \cong -115$ which is close to the total growth of Nd over the history of the earth. The lowest observed $\varepsilon_{Nd}(0)$ is about -30 and yields $C^{B}_{Nd} \cong 155$ ppm which is an excessively high value for possible detrital sources. It follows that the presence of detrital material in the manganese nodules cannot reasonably explain the observed differences between Pacific and Atlantic samples. If 20% by weight of a nodule is derived from an oceanic basalt with $\varepsilon_{Nd}(0) \cong +10$ and $C_{Nd} \cong 10$ ppm, we obtain a shift of 0.36 ε units. Some contributions from oceanic basalts and detrital material must obviously take place, but the above considerations show that the magnitude of their effects is likely to be less than an ε unit. We consider it most reasonable that the variations within an ocean basin reflect the dissolved content of Nd in different waters draining off of the various continental masses which are not completely mixed within the basin over the time scale for Nd deposition, and only a small contribution comes from oceanic magma sources.

Rapidly accumulating deposits of hydrothermal crusts and metalliferous sediments are associated with hydrothermal plumes ascending through MOR basalts. It has been demonstrated that hydrothermal leaching of MORB could supply the excess iron and manganese associated with hydrothermal crusts and metalliferous sediments from the observation that these and some other elements are depleted in the interiors of pillow basalts relative to their glassy margins (11). Zelanov (38) reported local concentrations of Fe and Mn hydroxides as high as 140 mg/liter of seawater in water samples collected near the mouths of hot springs associated with the submarine Banu Wuhu volcano, compared with normal seawater concentratio for these elements of less than 60 µgm/liter (5). Studies of Pb isotopes

in metalliferous sediments indicate a volcanogenic source for this element also (25, 39). However, only two hydrothermal sediment samples from the Pacific Ocean studied here (MS-1, HC-1) with $\varepsilon_{Nd}(0)$ about 2 ε units greater than the manganese nodules show any indication of a possible basaltic contribution to the Nd isotopes. Contributions from oceanic basalts to the Nd composition of hydrothermal crusts and metalliferous sediments can be demonstrated by comparing Mn/Nd ratios and $\varepsilon_{Nd}(0)$ in oceanic basalts with that in the hydrothermally deposited sediments. Typical MOR basalts have Mn/Nd ≅ 150 (Mn ≅ 1500 ppm, Nd ≅ 10 ppm) and $\varepsilon_{Nd}(0) \cong +10$ compared with a hydrothermal crust (HC-1) which has Mn/Nd ≅ 900 (Mn = 0.18% [29], Nd = 2.05 ppm) and $\varepsilon_{Nd}(0) = -1.4$. Mn/Nd ratios indicate that almost all of the Nd in the hydrothermal crust could in principle have a basaltic source. However, from the mixing equation presented earlier, using $\varepsilon_{Nd}(0) \cong +10$ for MORB and seawater with $\varepsilon_{Nd}(0) \cong -3$, we calculate that the maximum mass fraction of the hydrothermal crust (sample HC1) from basaltic sources must be less than about 5%. On the other hand, metalliferous sediment (MS-1) which has a much higher concentration of Nd (C_{Nd} = 20.7 ppm) must have a mass fraction of 25% of MORB to account for the observed ε value of -1.1 corresponding to a 2ε shift from our estimated ε value for Pacific seawater. If the Nd in these sediments is derived from Nd dissolved in hydrothermal solutions, then approximately 15% of the total Nd in these samples must come from Nd derived from basaltic sources. It is clear that the causes of variations within the oceans remain a major issue. Substantial contributions (~ 20%) to the dissolved load of Nd from primary oceanic sources may exist as assessed by these methods.

Sr isotopic data (this study, 6, 39) indicate that $\varepsilon_{Sr}(0)$ values

in these sediments are identical to seawater $\varepsilon_{Sr}(0)$ values as well. We conclude, therefore, in agreement with other authors (6, 25, 30, 39) that the source of REE, Sr, and possibly other elements is ambient seawater and was not dominated by local igneous sources. A small fraction of these elements (REE and Sr) may be added to hydrothermal crusts and metalliferous sediments possibly as a result of scavenging of seawater by Fe and Mn hydroxides when they are deposited from ascending solutions upon entering oxygenated seawater (28).

$f_{Sm/Nd}$ values have been measured for most samples. $f_{Sm/Nd}$ values for seawater range from -0.39 (this study) to -0.5 (2, 4). These values are typical of continental $f_{Sm/Nd}$ values (36). Manganese nodules and hydrothermal ferromanganese deposits exhibit a range of $f_{Sm/Nd}$ from about -0.2 to -0.4. MN-19 from Lake Oneida has an $\varepsilon_{Nd}(0)$ consistent with a continental source for its REE, yet has an extremely fractionated $f_{Sm/Nd}$ value (-0.159) relative to the probable $f_{Sm/Nd}$ value of its REE source material. The variation of $f_{Sm/Nd}$ exhibited by ferromanganese sediments is not consistent with a steady state model for the input versus output of elements in seawater. This indicates that complexities exist in the transport mechanisms of the REE into and out of seawater. Further study is needed in the mechanisms and rates of REE solution, transport, and precipitation before conclusions can be drawn from these variable enrichment factors.

T^{Nd}_{CHUR} ages have been calculated for the ferromanganese sediments and seawater analyzed here, using the measured $\varepsilon_{Nd}(0)$ and $f_{Sm/Nd}$ values (Table 3). These calculations assume the $f_{Sm/Nd}$ values are characteristic of the sources of REE. T^{Nd}_{CHUR} ages calculated are variable but have averages which are distinct for each ocean, with the Pacific samples having the

youngest ages and the Atlantic the oldest. Because it has been observed that $f_{Sm/Nd}$ is variable in ferromanganese sediments and not the same as the source values, these ages probably do not reflect the true source rock ages. If we use a typical $f_{Sm/Nd}$ value for a continental source of about -0.4 (36) we calculate an average age for the Atlantic Ocean samples of about 1.20 AE, 0.85 AE for the Indian Ocean, and for the Pacific samples an age of 0.35 AE. We also get a much tighter clustering of the calculated ages using a continental $f_{Sm/Nd}$ value which is consistent with the clustering observed for $\varepsilon_{Nd}(0)$ values. These ages are also younger than those calculated from measured $f_{Sm/Nd}$ values for the samples, but in either case, a distinctly older source for the REE in the Atlantic is clearly necessary to explain the difference between Atlantic and Pacific T^{Nd}_{CHUR} ages.

Reasonable constraints can be placed on the residence time of neodymium in seawater from the data presented here, along with available concentration data for Nd in crustal rocks and the dissolved load in river water. Approximate limits of the residence time of Nd (τ_{Nd}) can be calculated from variations of the Na/Nd ratios in crustal rocks (CR) and river water (RW) relative to seawater (SW) Na/Nd and the residence time of Na in seawater ($\tau_{Na} = 4.8 \times 10^7$ yr [5]). We can calculate τ_{Nd} from the equation

$$\tau_{Nd} = \tau_{Na}\left[\frac{(Na/Nd)_{CR}}{(Na/Nd)_{SW}}\right]$$

For $(Na/Nd)_{Cr} \cong 1000$ and $(Na/Nd)_{SW} = 3.5 \times 10^9$ as presented earlier, we get $\tau_{Nd} \cong 15$ years as a lower limit. Studies by several authors (5, 40, 41), however, indicate that only a small percentage of Nd eroded

from the continents enters the oceans as a dissolved component in river water. Using data from these authors, we get a range in $(Na/Nd)_{RW}$ from 3.0×10^4 to 1.5×10^5 (Na $\cong$ 6 ppm, Nd $\cong$ 40-200 $\times 10^{-6}$ ppm) and a range in τ_{Nd} from about 400 to 2000 years. Residence time calculations made by Goldberg et al. (2) based on fluxes of Nd into the oceans and the total dissolved content of Nd in the oceans yielded $\tau_{Nd} \cong 270$ years. Clearly, more studies are needed to determine the fluxes of the REE to the oceans to further define the residence time of Nd. Isotopic data presented here allows us to put one more constraint on τ_{Nd}. As mentioned earlier, we observe a tight clustering of $\varepsilon_{Nd}(0)$ in each ocean, but very marked distinctions between oceans. It is clear that to maintain these distinctions, the residence time of Nd must be considerably shorter than the mixing times between ocean basins. Beyond this, no other conclusions can be drawn from the data.

To obtain limitations on interocean mixing, we have for two ocean bodies 1 and 2 supplied by drainage from the respective land masses A and B, the following equations at steady state:

$$0 = \varepsilon_A J_{A1j} - \varepsilon_1 J_{13j} + \varepsilon_2 C_{2j} \dot{W}_{12} - \varepsilon_1 C_{1j} \dot{W}_{12}$$

$$0 = \varepsilon_B J_{B2j} - \varepsilon_2 J_{23j} - \varepsilon_2 C_{2j} \dot{W}_{12} + \varepsilon_1 C_{1j} \dot{W}_{12}$$

Here J_{A1j} and J_{B2j} are the fluxes of species j into oceans 1 and 2 from the sources A and B respectively. J_{13j} and J_{23j} are the rates of deposition of j (^{144}Nd in this case) from oceans 1 and 2 into the sediment layer, 3. $\dot{W}_{12}$ is the rate of exchange of water masses between 1 and 2. ε_1 and ε_2 are the ε values in each ocean. The ocean bodies are decoupled when $\dot{W}_{12} = 0$ which yields the condition $J'_{A1i} = J'_{13i}$ and $J'_{B2i} = J'_{23i}$ where the

primes indicate this special decoupled case for an arbitrary species i. If the systems are only weakly coupled, then assuming that $C_{1j} \cong C_{2j}$ we obtain

$$(\varepsilon_1-\varepsilon_A)\ J'_{13j} \cong (\varepsilon_2-\varepsilon_1)\ C_{1j}\ \dot{W}_{12}$$

$$(\varepsilon_2-\varepsilon_B)\ J'_{23j} \cong (\varepsilon_2-\varepsilon_1)\ C_{1j}\dot{W}_{12}$$

Using $$\frac{J'_{13j}}{C_{1j}W_1} = \frac{1}{\tau_{1j}}$$

for the mean residence time τ_{1j} in the decoupled water body of mass W_1, we get for the mixing time between 1 and 2 (τ_{12}) in terms of τ_{1j}:

$$\tau_{12} = \frac{W_1}{\dot{W}_{12}} \cong \frac{(\varepsilon_2-\varepsilon_1)\ \tau_{1j}}{(\varepsilon_1-\varepsilon_A)}$$

The difference between Atlantic and Pacific samples is $(\varepsilon_2-\varepsilon_1) \cong 8$ ε units. If $(\varepsilon_1-\varepsilon_A) \cong 2$ as estimated by the dispersion for the Pacific, this gives $\tau_{12} \cong 4\ \tau_{1j} \cong 4 \times 500$ years $\cong 2000$ years. Estimating ε_A is difficult from the available data and it is not evident that this approach can yield reliable results for interocean mixing times.

CONCLUSIONS

Previous workers (17, 18) have observed that a dominant continental component is necessary to explain the observed $\varepsilon_{Nd}(0)$ values for authigenic marine sediments. However, it is difficult to assess from the available data what the average $\varepsilon_{Nd}(0)$ value of continental material being supplied to the oceans is, and whether it varies from ocean to ocean. If we consider North American shale (NAS) with $\varepsilon_{Nd}(0) = -14.4$ (1) to represent average continental sources and $\varepsilon_{Nd}(0) = +10$ to represent average oceanic sources, then we can calculate that for the Atlantic Ocean there must

be at least a 90% contribution from continental sources and only 10% from MORB to account for the average $\varepsilon_{Nd}(0) \cong -12$ observed for this ocean. However, to account for variation of 2 ε units in seawater by the addition of Nd from MORB or oceanic volcanic sources would require a doubling of the oceanic contribution. At present it is not clear whether the observed variations which we attribute to seawater are a result of variations in the isotopic composition of the input of dissolved Nd from continental material or of major shifts in the proportion from oceanic sources. If we assume a similar minimum of 90% continentally derived Nd in the Pacific Ocean ($\varepsilon_{Nd}(0) \cong -3$) we calculate that the average $\varepsilon_{Nd}(0)$ value for continental sources for this ocean is about -4.5. This may not be an unreasonable value when the ages of the continental material being drained into the Pacific from Western North and South America are considered. There is, of course, considerably greater marine volcanic activity in the Pacific Ocean which could result in larger contributions to the REE from these sources. A minimum contribution of 55% continental Nd with NAS affinities is required to produce the observed $\varepsilon_{Nd}(0)$ values in authigenic sediments from the Pacific Ocean.

Data for MN-18 from the Scotia Sea indicate that $\varepsilon_{Nd}(0)$ in this sample is dominated by Nd with Pacific Ocean affinities in spite of a location more adjacent to the South Atlantic. This supports the view that ocean currents may be responsible for transporting REE from one water body to another. It may, therefore, be possible to determine ocean flow patterns and the effectiveness of such currents in transporting REE between water masses by measuring the Nd isotopic composition of seawater (either directly or indirectly) across observed Nd isotopic boundaries such as between the Scotia Sea and the South Atlantic Ocean.

Growth rates of deep-ocean manganese nodules are typically very slow. Typical growth rates average between 2-8 mm/10^6 years (34), making a nodule about 5 cm in diameter greater than 5 x 10^6 years old. The similarity of the $\varepsilon_{Nd}(0)$ values in manganese nodules with that measured for seawater suggests that it may be possible to trace variations of Nd through time by sampling several layers within a nodule corresponding to a large time span and therefore to provide a basis for monitoring the flow of ocean waters over times of 10^6 years.

REFERENCES

1. D. J. DePaolo and G. J. Wasserburg, Geophys. Res. Lett. 3, 249 (1976).

2. E. D. Goldberg, M. Koide, R. A. Schmitt, R. H. Smith, J. Geophys. Res. 68, 4209 (1963).

3. S. R. Taylor, Geochim. Cosmochim. Acta 28, 1273 (1964).

4. O. T. Høgdahl, B. T. Bowen, S. Melson, Advan. Chem. Ser. 73, 308 (1968).

5. H. D. Holland, The Chemistry of the Atmosphere and Oceans (J. Wiley and Sons, New York, 1978).

6. J. Dymond, J. B. Corliss, G. R. Heath, C. W. Field, E. J. Dasch, H. H. Veeh, Geol. Soc. Am. Bull. 84, 3355 (1973).

7. E. Bonatti, T. Kraemer, H. Rydell, in Ferromanganese Deposits on the Ocean Floor, D. R. Horn, Ed. (IDOE Publ. NSF, 1972).

8. D. Z. Piper, Geochim. Cosmochim. Acta 38, 1007 (1974).

9. G. Arrhenius and E. Bonatti, in Progress in Oceanography 3, M. Sears, Ed. (Pergamon Press, New York, 1965).

10. K. Bostrom and M.N.A. Peterson, Econ. Geol. 61, 1258 (1966).

11. J. B. Corliss, J. Geophys. Res. 76, 8128 (1971).

12. A. M. Ehrlich, Rare Earth Abundances in Manganese Nodules, Ph.D. Thesis (Massachusetts Institute of Technology, 1968).

13. M. L. Bender, in Ferromanganese Deposits on the Ocean Floor, D. R. Horn, Ed. (IDOE Publ. NSF, 1972).

14. D. J. DePaolo and G. J. Wasserburg, Geophys. Res. Lett. 3, 743 (1976).

15. R. K. O'Nions, P. J. Hamilton, N. M. Evensen, Earth Planet. Sci. Lett. 34, 13 (1977).

16. P. Richard, N. Shimizu, C. J. Allegre, ibid. 31, 269 (1976).

17. D. J. DePaolo and G. J. Wasserburg, Geophys. Res. Lett. 4, 465 (1977).

18. R. K. O'Nions, S. R. Carter, R. S. Cohen, N. M. Evensen, P. J. Hamilton, Nature 278, 435 (1978).

19. G. P. Glasby, in Ferromanganese Deposits on the Ocean Floor, D. R. Horn, Ed. (IDOE Publ. NSF, 1972).

20. _____, Mar. Chem. 1, 105 (1973).

21. W. Raab, in Ferromanganese Deposits on the Ocean Floor, D. R. Horn, Ed. (IDOE Publ. NSF, 1972).

22. D. S. Cronan, ibid.

23. _____, in Chemical Oceanography 5, J. P. Riley and R. Chester, Eds. (Academic Press, London, 1976).

24. R. K. Sorem and R. H. Fewkes, in Marine Manganese Deposits, G. P. Glasby, Ed. (Elsevier, Amsterdam, 1977).

25. M. Bender, W. Broecker, V. Gornitz, U. Middel, R. Kay, S. Sun, P. Biscaye, Earth Planet. Sci. Lett. 12, 425 (1971).

26. M. R. Scott, R. B. Scott, P. A. Rona, L. W. Butler, A. J. Nalwalk, Geophys. Res. Lett. 1, 355 (1974).

27. W. S. Moore and P. R. Vogt, Earth Planet. Sci. Lett. 29, 349 (1976).

28. E. Bonatti, A. Rev. Earth. Planet. Sci. 3, 401 (1975).

29. J. B. Corliss, M. Lyle, J. Dymond, K. Crane, Earth Planet. Sci. Lett. 40, 12 (1978).

30. J. R. Toth, Deposition of submarine hydrothermal manganese and iron, and evidence for input of volatile elements to the ocean, M. S. Thesis (Oregon St. U., unpubl., 1977).

31. D. A. Papanastassiou, D. J. DePaolo, G. J. Wasserburg, Proc. Lunar Sci. Conf. 8th, 1639 (1977).

32. D. A. Papanastassiou and G. J. Wasserburg, Earth Planet. Sci. Lett. 17, 324 (1973).

33. G. J. Wasserburg, D. A. Papanastassiou, E. V. Nenow, C. A. Bauman, Rev. Sci. Instr. 40, 288 (1969).

34. T. L. Ku, in Marine Manganese Deposits, G. P. Glasby, Ed. (Elsevier, Amsterdam, 1977).

35. J. Greenslate, Geophys. Res. Lett. 5, 237 (1978).

36. M. T. McCulloch and G. J. Wasserburg, Science 200, 1003 (1978).

37. D. S. Cronan, in Marine Manganese Deposits, G. P. Glasby, Ed. (Elsevier, Amsterdam, 1977).

38. K. K. Zelanov, Doklady Akad. Nauk SSSR 155, 94 (1964).

39. E. J. Dasch, J. R. Dymond, G. R. Heath, Earth Planet Sci. Lett. 13, 175 (1971).

40. J.-M. Martin, O. Høgdahl, J. C. Philippot, J. Geophys. Res. 81, 3119 (1976).

41. J.-M. Martin and M. Meybeck, Mar. Chem. 7, 173 (1979).

42. D. A. Papanastassiou and G. J. Wasserburg, Geophys. Res. Lett. 5, 595 (1978).

43. O. Eugster, F. Tera, D. S. Burnett, G. J. Wasserburg, J. Geophys. Res. 75, 2753 (1970).

44. G. P. Russ III, Neutron stratigraphy in the lunar regolith, Ph.D. Thesis (California Institute of Technology, 1974).

45. D. J. DePaolo, Study of magma sources, mantle structure and the differentiation of the Earth from variations of $^{143}Nd/^{144}Nd$ in Igneous Rocks, Ph.D. Thesis (California Institute of Technology, 1978).

46. A. O. Nier, Phys. Rev. 77, 789 (1950).

APPENDIX 1

CHEMICAL SEPARATION OF Sm AND Nd

Separation of Sm and Nd is accomplished by using a method similar to that described by Eugster et al. (43). The method has been described in detail by Russ (44) and DePaolo (45) and only essential details of the procedure will be reproduced here. Details of sample preparation have been discussed briefly in the previous section and will not be considered here.

Two ion exchange columns are used to separate Sm and Nd. The first column is constructed of quartz glass with a 1 cm inside diameter. This is filled to a height of 17 cm with Dowex 50-8x, 100-200 mesh cation exchange resin. Prior to an elution, the resin is prepared by passing 300 ml of high purity 4N HCl through the column in 100 ml portions, followed by 10 ml of 1.5N HCl. 1.5 N HCl increases the pH on the upper part of the column. This results in the sample being partitioned into the resin and thusly being held onto the top of the column. Dissolved samples are dried down and then taken up in 2 ml of 1.5 N HCl. This solution is then centrifuged in a quartz glass tube and loaded onto the top of the resin with a disposable pipette. Care should be taken to avoid getting sample on the reservoir at the top of the column. The sample is then allowed to pass through under its own weight. When all of the solution is onto the resin, 2 ml of 1.5 N HCl is poured onto the column in 1 ml aliquants to rinse the column down in order to get all of the sample onto the resin, allowing each time for the liquid to pass into the resin. All of the sample now should be on the top of the resin, and the elution is begun. REE are eluted through the column using 4N HCl. A two-step procedure may be used

also if it is desired to separate Rb and Sr also. In this case, the elution is started with 2.5 N HCl. Rb and Sr are moved through the column more rapidly than the REE and allows complete separation of these elements from each other and the REE. The elution can then be completed with 4N HCl to obtain the REE. A typical elution curve is shown in figure A1-1 showing the separation of Sr, Ba, and REE. There is some separation of the REE, so a large fraction is collected to ensure that all of the Sm and Nd are recovered. Fractions are determined by passing radioactive tracers of the desired elements through the column. The fractions containing Rb and Sr can be dried down and loaded directly onto a filament for mass spectrometry. The solution containing the REE fractions is also dried down before loading it onto the second column where REE will be separated from each other and Ba.

The second ion exchange column is made of thick-walled Pyrex tubing. The column is 33 cm long with a 0.2 cm inside diameter and an 8 ml reservoir above. The base of the column is inserted into a teflon nipple which contains a small disc of filter paper. The column is filled with resin to a height of about 30 cm, and the resin is held in the column by the filter paper at the bottom. The resin is discarded after each elution. The top of the column is connected to a Tygon tube by the use of a ground glass ball joint. This end of the tubing has a socket connector and a teflon stop-cock. The Tygon tube is attached to two 2 liter bottles half-filled with water which are connected by approximately 3 m of Tygon tubing and suspended one about 2.5 m above the other to provide air pressure at the top of the column to speed up the rate at which eluant passes through the column. During the elution, the amount of effluent leaving the column is monitored with a photo-electric drop counter.

FIGURE A1-1

Typical elution curves for Sr, REE, and Ba from first cation exchange column.

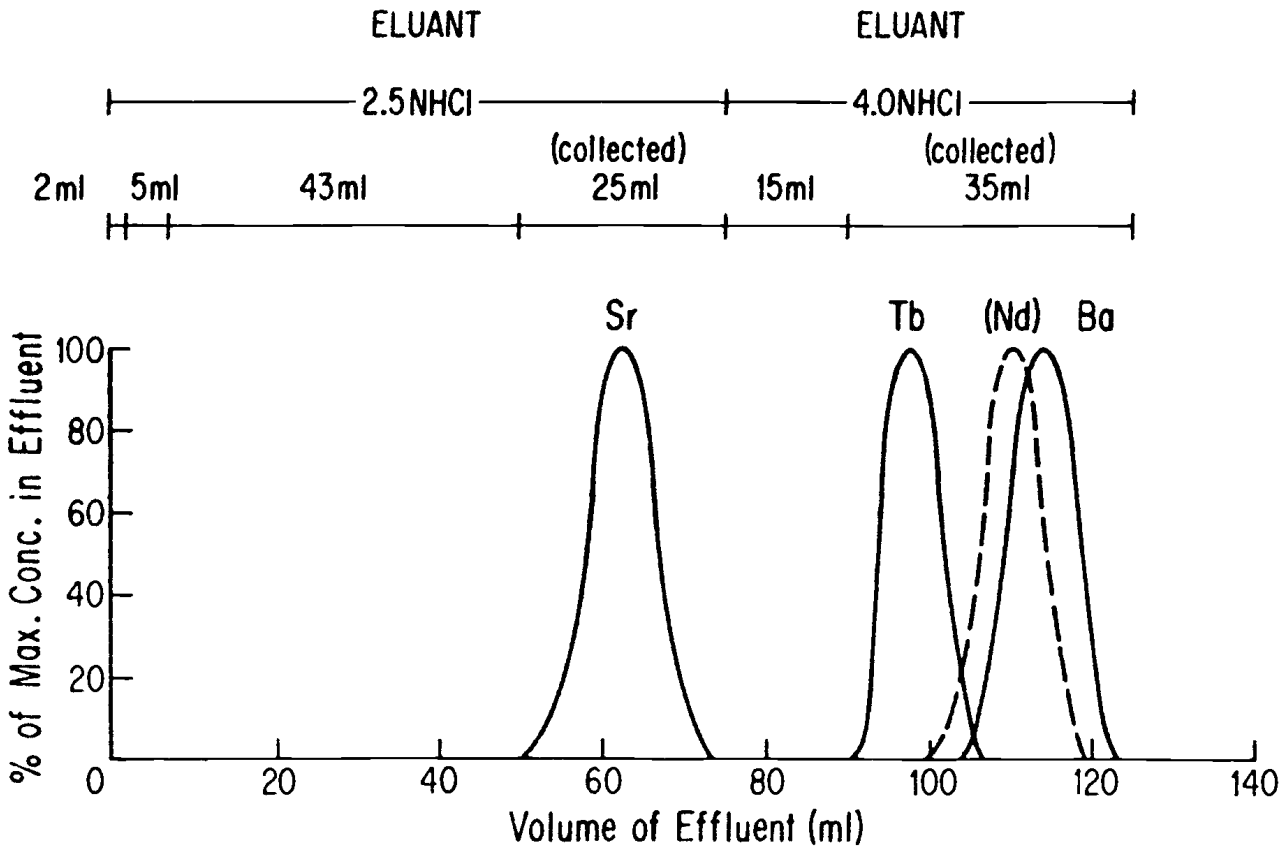
ELUANT
ELUANT
2.5NHCl
4.0NHCl
2ml
5ml
43ml
(collected)
25ml
15ml
(collected)
35ml
Sr
Tb
(Nd)
Ba
% of Max. Conc. in Effluent
100
80
60
40
20
0
20
40
60
80
100
120
140
Volume of Effluent (ml)

Fig. A1-1

Resin used in this column requires special preparation before being loaded into the column. Enough resin for 50-100 elutions is placed in a large column (about 30 cm x 2 cm) with a 500 ml reservoir. The resin is then rinsed by passing 1 liter of distilled water through it, followed by 1 liter of 4N HCl and then another liter of distilled water. Next, 1 liter of 0.4 M 2-methyllactic acid with pH adjusted to 4.7 is passed through, followed once again by 1 liter of distilled water. The top 1/3 of the resin is then discarded and the remainder is stored in a polyethylene bottle under water.

The 2-methyllactic acid is prepared by weighing out 0.4 moles of the acid which is obtained as a solid and dissolving this in one liter of distilled water. The pH is adjusted by adding concentrated NH_4OH prepared by bubbling NH_4 gas through distilled water. The solution acts as a buffer, keeping the pH stable over long periods.

Samples are eluted through the second column using 0.2 M 2-methyllactic acid with pH adjusted to about 4.6. The resin used for the previous sample is removed first with a 40 cm long, 1.5 mm outside diameter capillary tube connected to a 5 or 10 cc disposable syringe. After the resin has been sucked out, the column reservoir should be filled a few times with water and drawn out through the capillary. The tip of the capillary tube should be as close to the bottom of the column so the water completely rinses the column. Some air should also be drawn through the filter paper to remove particles of resin. Care should be taken to avoid damage to the filter paper. When rinsing is complete, some H_2O is left in the column and new resin is added. The storage bottle is shaken and resin withdrawn with a clean pipette and transferred to the column reservoir. The pipette should not touch the top of the column during the

expulsion of the resin as the pipette will probably be needed again to get more resin to fill the column to the top of the neck below the reservoir. The resin is allowed to settle about two hours into the column. When the resin has settled, the pipette is used to remove any excess resin and water above the top of the capillary. The reservoir is then filled with 0.2 m methyllactic acid (preparation described earlier) and allowed to drip through under its own weight overnight. The drop counter should be activated during this time and 100 drops should pass through the column before starting the elution. After this, the pipette is used to adjust the resin height to 30 cm and remove excess eluant. The column is then filled with distilled water to the top of the capillary and is passed through under air pressure. Care must be taken to remove the air pressure just as the last water reaches the top of the resin, or the resin will be dried out by the flow of air and then the resin must be removed and the process started over.

At this point, the sample is ready to be loaded onto the column. When loading the sample, care should be taken to get all the sample on the top of the resin before starting the elution in order to have a good separation of Sm and Nd. The dried sample containing the REE collected from the first column is dissolved in 2 drops of 0.75 N HCl, using a dispenser which expells fairly uniform drop sizes. It is then loaded onto the column using a clean pipette. The pipette tip is lowered to the bottom of the reservoir. The sample is put onto the column by touching the tip of the pipette to the bottom of the reservoir and slowly expelling the sample so it runs down the capillary. Care should be taken to avoid touching the pipette tip to any other surface of the reservoir at any time. If this becomes mixed with eluant, heavy REE will be found in every fraction

collected. This solution is then passed through under pressure as with the water. Another two drops of 0.75 N HCl are added to the sample beaker and also added to the column in the same manner and allowed to pass through under pressure. Most of the sample is now on the resin, but some still remains on the bottom of the reservoir and the sides of the capillary.

About 8-10 ml of eluant is poured into a clean teflon beaker, and a clean pipette is then used to draw up about 0.5 ml of eluant. The column is filled with eluant to the top of the neck as before. The eluant should be used to rinse the walls of the reservoir and column which have come in contact with sample so as to get all sample onto the column. Keep the remaining eluant in the pipette. Turn on the drop counter and set it to zero and then begin passing the eluant through the resin under pressure, stopping the flow as before when the liquid is about to run out. Repeat this process again. After this, fill the capillary a third time and then pour the remaining eluant from the beaker into the column reservoir. Never return the pipette used for rinsing the column down to the beaker containing eluant. If more is needed, use a clean pipette. After the reservoir has been filled, start passing the eluant through under air pressure. The fractions containing Sm and Nd are collected in clean teflon beakers and dried down under a heat lamp. A metal base should be used as the methyllactate is rather involatile. The sample should be completely dry before removing it from the heat.

The second cation exchange column is calibrated by the use of radioactive tracers (^{152}Eu, ^{154}Eu, ^{151}Sm, and ^{147}Nd). ^{151}Sm can be omitted and the Sm cut calculated from the Eu and Nd curves. These tracers are eluted through the column in the same manner as described above. Drops

are collected by a fraction collector which can be operated by the drop counter. ^{147}Nd has a short half-life ($\tau_{1/2}$ = 11 days) and must be ordered specially from a radiochemical supplier such as Oak Ridge. A typical elution curve is shown in figure A1-2. Separation of the REE is very efficient. The Nd fraction can be better than 99.95% pure as determined from mass spectra. Purity is mostly affected by sample loading procedures onto the first column. If the eluant has been contaminated with sample, for example, the Nd cut would be likely to have a sizeable Sm component present.

FIGURE A1-2

Typical elution curves for Eu, Sm, and Nd from second cation exchange column. Note the excellent separation of Sm from Nd.

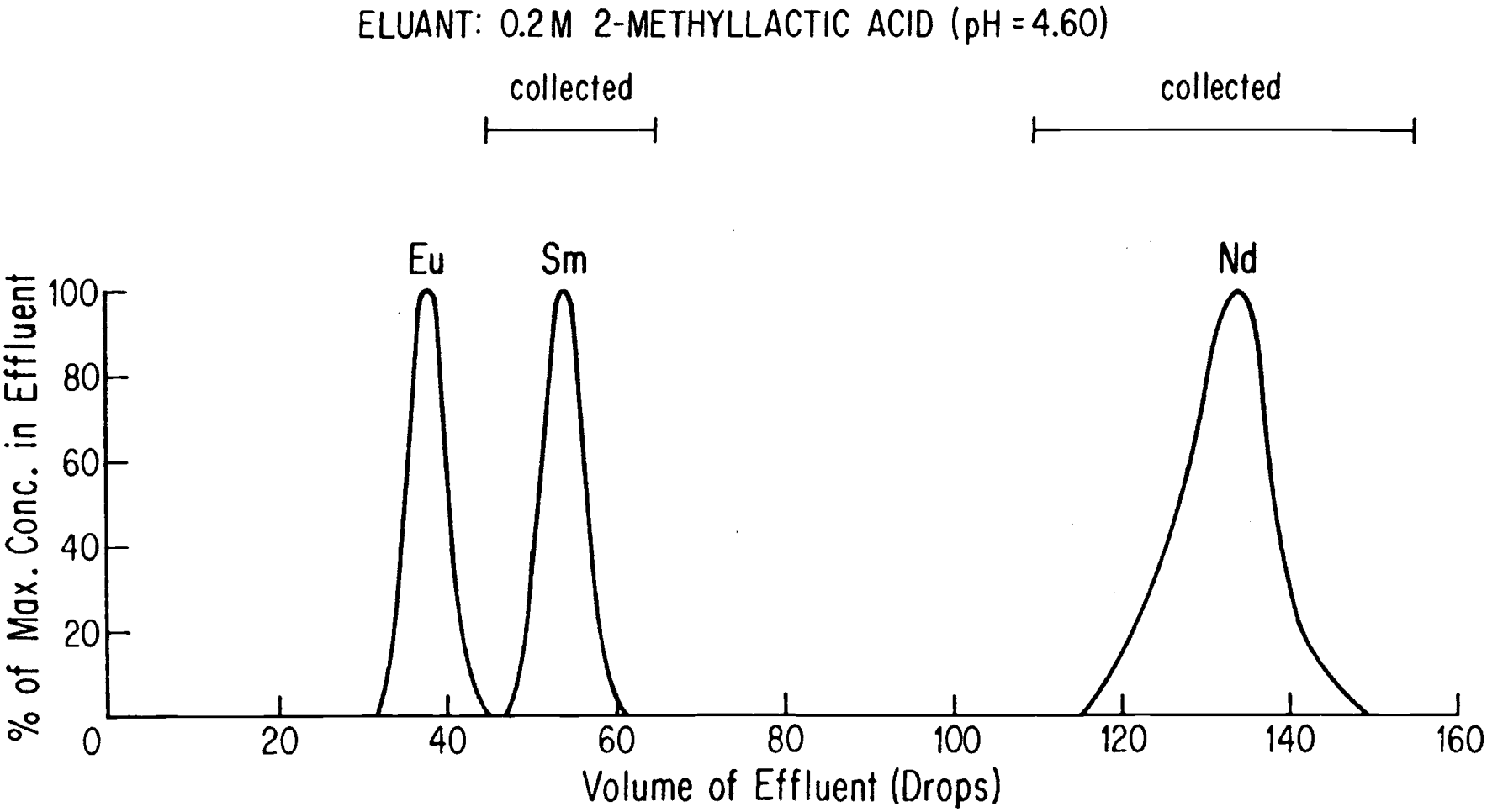
ELUANT: 0.2 M 2-METHYLLACTIC ACID (pH = 4.60)
collected
collected
Eu
Sm
Nd
% of Max. Conc. in Effluent
100
80
60
40
20
0
20
40
60
80
100
120
140
160
Volume of Effluent (Drops)

Fig. A1-2

APPENDIX 2

MASS SPECTROMETRY

Nd samples are loaded onto flat Re filaments for isotopic analysis. Polyethylene tubing (0.023" I.D.) connected to a syringe is used to transfer the sample to the filament. The tubing is first cleaned by drawing 4N HCl up into it and then expelling it 3 or 4 times. The outside of the tubing should also be rinsed down with 4N HCl from a squeeze bottle. Then approximately 5 to 10 µl of 1.5 N HCl are drawn up into the tubing, and this is expelled onto the sample and the solution is allowed to stand for a few minutes. Then the tubing is used to scrape the sample up from the bottom of the beaker and to mix up the solution. When the sample is completely dissolved the solution should have a pale brown color. At this point the entire solution is drawn up into the tubing and its volume is determined by measuring the length of the solution in the tubing. The solution is then expelled and an amount equivalent to about 200 nanograms of Nd is drawn up. This is then loaded onto the center 1/4 of the filament in several very small drops. Each drop is evaporated by passing a current of 0.5A through the filament. If after the entire solution has been placed on the filament and evaporated the sample is distributed unevenly, the tip of the tubing can be used to gently spread the sample around and even it out. Care must be taken to make sure the filament is cold when the tubing is touched to it, otherwise the tubing will melt on the filament and cause deposits which can affect the beam stability. When the sample is satisfactorily loaded on the filament the current is increased gradually up to about 1.8-2.0A in order to oxidize the Nd to Nd_2O_3. As the current is increased

the organic residue burns away; the sample appears white or bluish-white when completely oxidized. During this process the Re filament may also become somewhat oxidized and some recrystallization may be evident.

After the filament has been loaded into the mass spectrometer source, it is heated up to a temperature of about 1250°C over a period of a few hours. It can be heated quickly up to 1000°C over about 10 minutes, but should then be heated more slowly up to the running temperature. At some point during the heating the signal may begin to grow by itself, without further increasing the filament temperature. However, usually the signal will not continue to grow throughout the run.

The efficiency of formation of Nd O^+ ions from the Nd_2O_3 is remarkably high, so that a sample of about 30 ng will provide a $^{144}Nd\ ^{16}O^+$ beam of 8×10^{-12}A for a period of several hours. Generally, the ratio of Nd O^+ ions appearing at the collector of Nd atoms originally loaded onto the filament is about 0.05. Usually about 100 ng of Nd is loaded onto the filament and the intensity of the ^{144}Nd O beam is kept between 7 and 9.5×10^{-12}A during data acquisition. This intensity is chosen so that all the isotopes can be measured on the same range of the digital voltmeter (DVM) to avoid scale corrections. For the $10^{11}\Omega$ feedback resistor this results in voltages ranging in intensity from $\sim$ 0.2V for ^{148}Nd O^+ and ^{150}Nd O^+ up to 1.0V for ^{142}Nd O^+. For samples containing high enough concentrations of Nd, about 500-700 ng of Nd can be loaded and the ion beam intensity increased by a factor of 10. In this case the $10^{10}\Omega$ feedback resistor can be used resulting in the same voltages.

A typical Nd O^+ mass spectrum is shown in Figure A2-1. For a source slit width of 0.010" and collector slit width of 0.025" the peak

FIGURE A2-1

Strip chart recording of a magnetic field scan of the Nd mass region taken during a run. $^{154}Sm\ O^+$ can barely be detected at mass 170; in this run the peak at mass 170 is about 0.2mV compared to 8.5 volts for $^{144}Nd\ O^+$, a ratio of 2.4×10^{-5}. The oxygen isotope spectrum can be seen clearly at mass 166, 167, and 168. The apparent longer beam tails on the high mass side of all the peaks are due to the fairly long time necessary for the decay of the peak current in the feedback resistor; scan is from right to left (low to high mass). Note that there is no detectable $Pr\ O^+$ or $Ce\ O^+$ in the spectrum; $La\ O^+$ does not interfere.

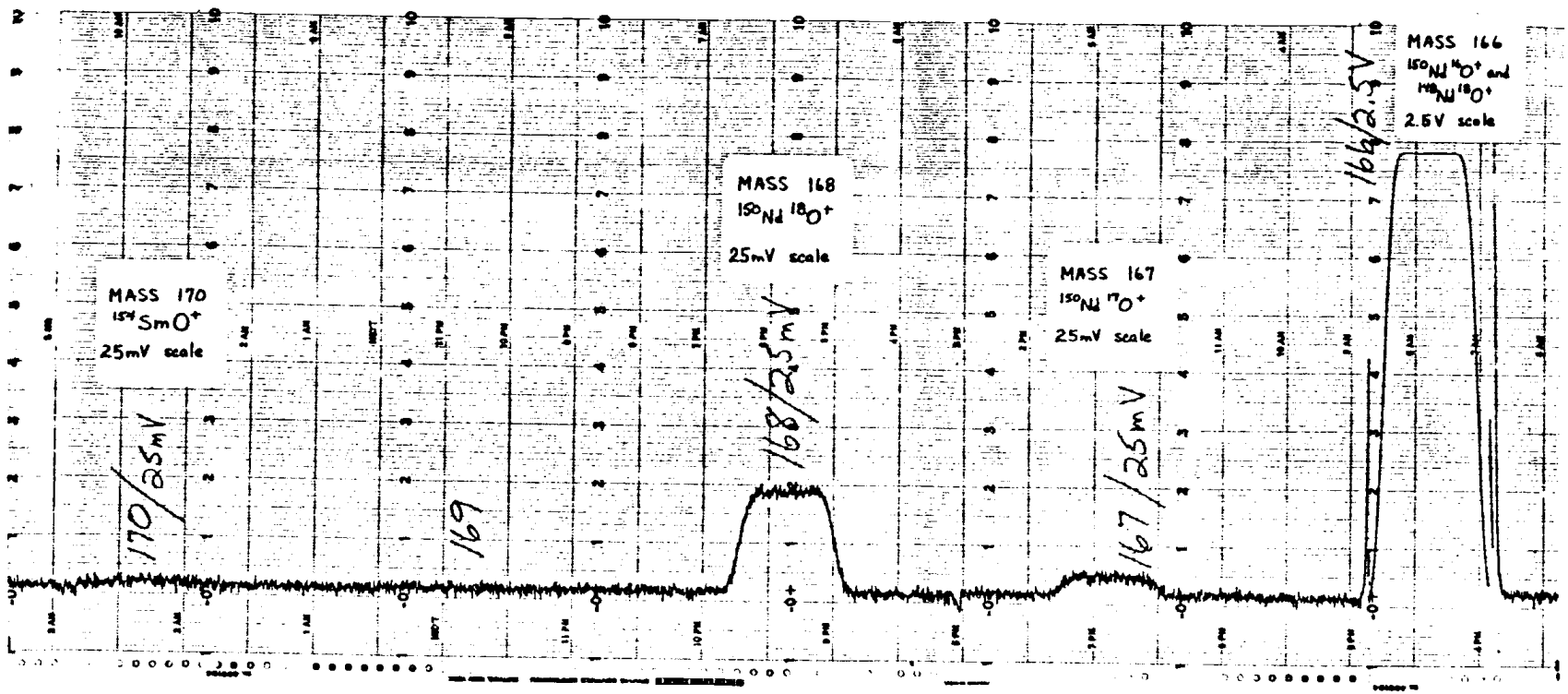
MASS 170
$^{154}SmO^+$
25mV scale
MASS 168
$^{150}Nd\,^{18}O^+$
25mV scale
MASS 167
$^{150}Nd\,^{17}O^+$
25mV scale
MASS 166
$^{150}Nd\,^{16}O^+$ and
$^{148}Nd\,^{18}O^+$
2.5V scale
170/25mV
169
168/25mV
167/25mV
166/2.5V

Fig. A2-1

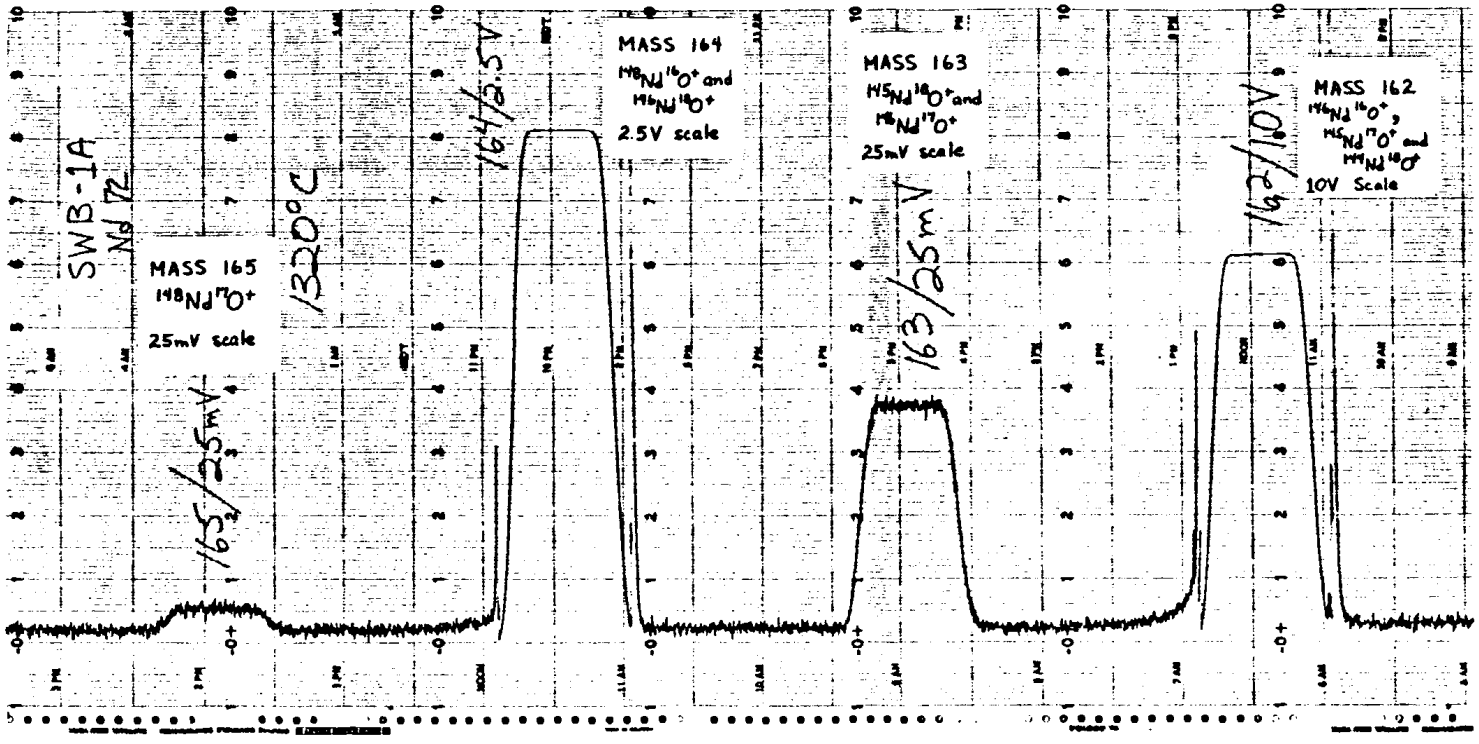
SWB-1A
Nd 72
1330°C
MASS 165
$^{148}Nd^{17}O^+$
25mV scale
165/25mV
MASS 164
$^{148}Nd^{16}O^+$ and
$^{149}Nd^{16}O^+$
2.5V scale
164/2.5V
MASS 163
$^{145}Nd^{18}O^+$ and
$^{148}Nd^{17}O^+$
25mV scale
163/25mV
MASS 162
$^{146}Nd^{16}O^+$,
$^{145}Nd^{17}O^+$ and
$^{144}Nd^{18}O$
10V Scale
162/10V

Fig. A2-1

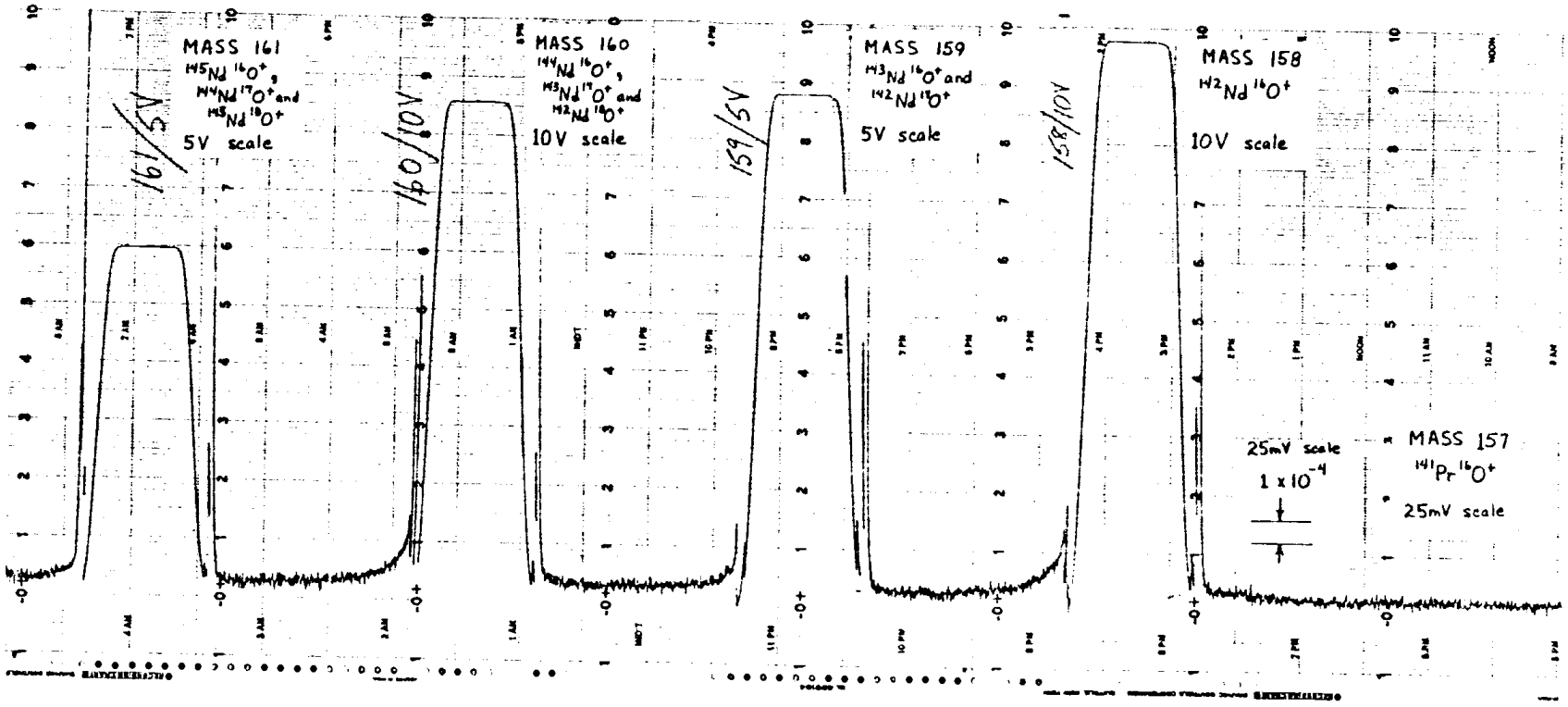
MASS 161
$^{145}Nd\,^{16}O^+$,
$^{144}Nd\,^{17}O^+$ and
$^{143}Nd\,^{18}O^+$
5V scale
161/5V
MASS 160
$^{144}Nd\,^{16}O^+$,
$^{143}Nd\,^{17}O^+$ and
$^{142}Nd\,^{18}O^+$
10V scale
160/10V
MASS 159
$^{143}Nd\,^{16}O^+$ and
$^{142}Nd\,^{17}O^+$
5V scale
159/5V
MASS 158
$^{142}Nd\,^{16}O^+$
10V scale
158/10V
25mV scale
1×10^{-4}
MASS 157
$^{141}Pr\,^{16}O^+$
25mV scale

Fig. A2-1

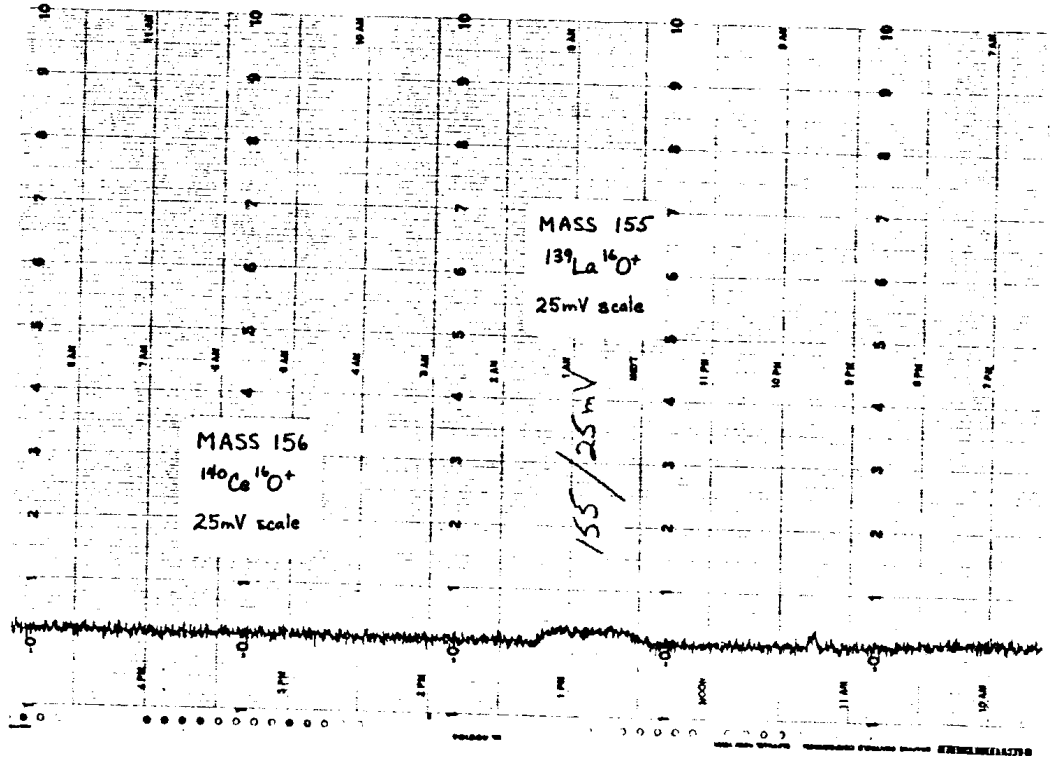
MASS 156
$^{140}Ce^{16}O^{+}$
25mV scale
MASS 155
$^{139}La^{16}O^{+}$
25mV scale
155/25mV

Fig. A2-1

tops are flat to 1 part in 10^5 of the peak intensity for ±1.5 gauss from the peak center (equivalent to about ±0.07 mass units). Background (zeros) are measured at 9.0 gauss from the peak centers (0.36 mass units). The background at ±0.36 m.u. is offset by 0.005% to 0.007% of the peak intensity from the value measured with the beam off. This proportional offset is approximately equal for all isotopes and thus cancels out in the measurement of isotope abundance ratios. Possible spectral interferences are monitored at mass 156 ($^{140}Ce\ O^+$), mass 157 ($^{141}Pr\ O^+$) and mass 170 ($^{154}Sm\ O^+$) using an electron multiplier. Normally the peaks at these masses are < 10^{-5}, 10^{-5} to 10^{-3}, and $5x10^{-6}$ to 10^{-4} respectively of the $^{144}Nd\ O^+$ peak, and no corrections to the Nd isotope ratios due to interfering species are necessary. Corrections are made for interference from Sm if the peak at mass 170 is greater than $5x10^{-5}$ of the $^{144}Nd\ O^+$ peak, however, this correction does not affect the measured $^{143}Nd/^{144}Nd$. La O^+ (mass 155) and sometimes Ba^+ (mass 138) are also detected in the spectrum at intensities of about 10^{-3} to 10^{-4} of $^{144}Nd\ O^+$ but do not interfere.

Nd ion beam intensity ratios are calculated relative to $^{144}Nd\ O^+$. At each mass the peak intensity and the background on each side of the peak are measured. At each position the signal is integrated for 1 second. The amount of time between the start of the DVM integration at the first zero position and the start of the DVM integration at the peak position, and between the peak and the second zero integration at each mass is kept constant at 2.94 seconds. The peak intensities are measured in the sequence $^{144}Nd\ O^+$, $^{143}Nd\ O^+$, $^{142}Nd\ O^+$, $^{150}Nd\ O^+$, $^{148}Nd\ O^+$, $^{146}Nd\ O^+$, $^{145}Nd\ O^+$ which corresponds to masses 160, 159, 158, 166, 164, 162, and 161.

Data are taken in sets of 10 mass scans, averaged, corrected for oxygen isotope composition, and then corrected for mass discrimination. Oxygen isotope corrections were made using the composition given by Nier (46). The procedure used for making the oxygen corrections is outlined in Table A2-1. Mass discrimination corrections were made by normalizing to $^{150}Nd/^{142}Nd = 0.2096$, which is the average value measured in the Lunatic I mass spectrometer (Wasserburg et al. [33]). The ratio $^{150}Nd/^{142}Nd$ is used for the determination of mass fractionation because the difference of 8 mass units for these isotopes minimizes the error in determining the fractionation factor per mass unit. The fractionation factor per mass unit α is calculated from:

$$\alpha = \frac{1}{8} \frac{(^{150}Nd/^{142}Nd)_{meas}}{0.2096} - 1$$

Each measured isotope ratio $(^{i}Nd/^{144}Nd)_{meas}$ is then corrected for mass fractionation using the formula:

$$(^{i}Nd/^{144}Nd)_{corr} = (^{i}Nd/^{144}Nd)/[1 + \alpha(i-144)]$$

In many cases Nd isotopic measurements are made on samples to which ^{150}Nd tracer has been added. The ^{150}Nd tracer is approximately 95% ^{150}Nd. The small amounts of the other Nd isotopes in the tracer significantly change the measured isotope ratios so that corrections must be made. These corrections are made using the measured isotopic composition of the tracer. This measurement is quite precise, but additional uncertainty must be added to the measured ratios due to the inability to precisely measure the instrumental mass discrimination during the measurement of the tracer. As an example of the magnitude of corrections

Table A2-1: Oxygen isotope corrections to measured Nd O^+ isotope ratios.*

A. $143^* = (159/160)_m - (158/160)_m R_{17}$

$144^* = 1 - (158/160)_m R_{18} - 143^* R_{17}$

$145^* = (161/160)_m - 143^* R_{18} - 144^* R_{17}$

$146^* = (162/160)_m - 144^* R_{18} - 145^* R_{17}$

$148^* = (164/160)_m - 146^* R_{18}$

$150^* = (166/160)_m - 148^* R_{18}$

B $142/144 = (158/160)_m/144^*$

$143/144 = 143^*/144^*$

$145/144 = 145^*/144^*$

$145/144 = 146^*/144^*$

$148/144 = 148^*/144^*$

$150/144 = 150^*/144^*$

where: $R_{17} \equiv {}^{17}O/{}^{16}O$; $R_{18} \equiv {}^{18}O/{}^{16}O$; m denotes measured (oxide) mass abundance ratio.

*Numbers refer to the masses of the Nd isotopes and the masses of the Nd O^+ isotopic species. Thus 142/144 is equivalent to $^{142}Nd/^{144}Nd$ and 158/160 is equivalent to $^{142}Nd\ O/^{144}Nd\ O$.

due to the tracer composition the net correction to $^{143}Nd/^{144}Nd$ under normal spiking conditions (^{150}Nd-tracer added equal to twice ^{150}Nd in sample) is approximately (0.5±0.0003)% where the uncertainty is due to uncertainty in the tracer composition. The added uncertainty to $^{143}Nd/^{144}Nd$ from this effect is therefore negligible. Due to the presence of the ^{150}Nd tracer, $^{150}Nd/^{142}Nd$ cannot be used to correct for instrumental mass discrimination. Therefore, in these runs Nd isotopic ratios were normalized to $^{146}Nd/^{142}Nd = 0.636155$. This is equivalent to normalizing to $^{150}Nd/^{142}Nd = 0.2096$ for the unspiked samples (DePaolo and Wasserburg [14]) and is essentially the average value that is measured in the Lunatic I mass spectrometer (Wasserburg et al. [33]) if no correction is made for mass fractionation. The $^{146}Nd/^{142}Nd$ ratio is used for the determination of fractionation because this ratio still provides a difference of 4 mass units, involves abundant Nd isotopes, and the contributions to ^{142}Nd and ^{146}Nd from the ^{150}Nd tracer are small.